Table 1
Frequency of sequence patterns of 13 bp nucleotides up–downstream of the target HCV Core a.a.70.

Pattern	Sequences (544–556 bp)*	Core a.a.70	Core a.a.70-type	Frequency
1	5′-ctcgc cgg cccga-3′	Arginine	Wild-type	45/87; 51.71%
2	5′-ctcgc cg*a* cccga-3′	Arginine	Wild-type	8/87; 9.20%
3	5′-ctcgc c*ag* cccga-3′	Glutamine	Mutant-type	25/87; 28.74%
4	5′-ctcgc c*aa* cccga-3′	Glutamine	Mutant-type	6/87; 6.90%
5	5′-*Y*tcgc cgg cccga-3′	Arginine	Wild-type	1/87; 1.15%
6	5′-ctcgc cg*t* cccga-3′	Arginine	Wild-type	1/87; 1.15%
7	5′-ctcgc c*at* cccga-3′	Histidine	Mutant-type	1/87; 1.15%

Direct nucleotide sequence analysis of the 87 patients with HCV was performed to determine mutation patterns. The letters in bold italics indicate the mutation in the target sequence to the probes, which were substitution to pattern 1 (51.71%; the most major sequence pattern in this study), and the underlines indicate three bases of the core a.a. 70 codon.

* The nucleotide position (bp) was numbered according to the full-length genome sequence of HCV genotype 1b strain NC1, GenBank accession number AB691953.1. *Y*: *c* + *t*.

(final concentration, 500 nM each), and 5 μL of cDNA. Droplets were generated using the droplet generator (DG) with 70 μL of DG oil per well with a DG8 cartridge and cartridge holder, 20 μL of PCR reaction mix, and a DG8 gasket. Droplets were dispensed into each well of a 96-well PCR plate by aspirating 40 μL from the DG8 cartridge. The PCR plate was subsequently heat-sealed with foil and placed in a PCR thermal cycler Mastercycler® Nexus gradient (Eppendorf AG, Hamburg, Germany). The cycling conditions were as follows: an initial denaturation cycle of 10 min at 95 °C, followed by 45 cycles of denaturation for 30 s at 94 °C, annealing for 2 min at 49 °C, extension for 1 min at 72 °C, and a final incubation for 10 min at 98 °C. After cycling, the droplets were immediately analyzed or stored at 4 °C, and the PCR plates were transferred to the QX100 Droplet Reader (Bio-Rad). The ddPCR workflow and data analysis were performed as described previously (Pinheiro et al., 2012). Positive and negative amplicon-containing droplets (accepted droplets) were discriminated using the fluorescence amplitude threshold, as determined with QuantaSoft software (Bio-Rad). The frequency (%) of mutations in Core a.a.70 was determined by calculating the ratio of mutant versus wild-type + mutant copies.

2.7. HCV RNA quantitation

HCV RNA values were quantitated using the COBAS TaqMan® HCV Test (Roche Diagnostics).

2.8. Quality control

To avoid generating false positives, general guidelines published online (Roche-PCR-Chapters, 2009) were applied. The procedure included the physical separation of areas for extraction, PCR setup and amplification/detection, and use of filtered tips. To monitor contamination, one sample of PBS for every 32 samples was processed and extracted. In addition, a template control (water) was added to the PCR plate. Over the course of the study, no false positives were detected.

2.9. Statistical analysis

The linear range of the ddPCR assay was determined by plotting the data and comparing them with a line of the same slope. Pearson's correlation coefficients were calculated using Microsoft Excel (Microsoft Corp., Redmond, WA, USA), and linear regression analyses were performed and displayed as scatter plots using GraphPad Prism 6.0 software (GraphPad Software, Inc., San Diego, CA, USA).

3. Results

3.1. Mutations in Core a.a.70 determined by direct nucleotide sequencing

Wild-type and mutant sequences were detected in 55 and 32 samples, respectively (Table 1). The elution profiles for five samples indicated the presence of more than one sequence (Fig. 1). Even after seven analyses, the samples represented two mutant strains and two wild-type strains; however, it was difficult to determine whether sample 1 was a mutant. This sample was eventually determined as a mutant by direct sequences. UDPS analysis of the viral genomic region that encodes the HCV Core protein in clinical samples recently showed a mixture of mutant and wild-type sequences in Core a.a.70 in 71 of 79 (89.9%) cases, and the ratio of mixtures increased as liver disease advanced to liver cirrhosis and HCC (Miura et al., 2013). Therefore, it was considered necessary to develop a more sensitive assay for the quantitation of mutations in Core a.a.70 to predict the progression of liver disease.

3.2. Optimization of the ddPCR assay

It was essential to determine the optimum annealing temperature for the ddPCR assay to detect mutations in Core a.a.70. Therefore, plasmid-DNA (100,000 copies/well) was annealed at the following temperatures: 43.0, 43.5, 44.6, 46.5, 48.9, 51.3, 53.7, 56.1, 58.5, 60.4, 61.5, and 62.0 °C. The amplitudes of FAM (mutant, Fig. 2A) and VIC (wild type, Fig. 2B) signals are displayed as rain plots. In this example, the chosen annealing temperature was 49 °C.

3.3. Specificity

The specificity of the assay was determined using samples containing wild-type (160,000 copies/well) or mutant plasmids (160,000 copies/well). Subsequent experiments were conducted at 49 °C for 45 cycles (Fig. 2C and D). No positive droplet was detected when using FAM in the presence of wild type plasmid, and when using VIC in the presence of mutant plasmid For wild-type and mutant plasmid ($n = 4$; FAM: Fig. 2C and VIC: Fig. 2D, rain plot). The rate of false positives was 0% for both mutant and wild-type plasmids.

3.4. Sensitivity and linearity of detection

The ddPCR assay was used to determine the relative ratios of mutant and wild-type sequences in mixed infections. Linearity and precision of the ddPCR assay were in agreement over a

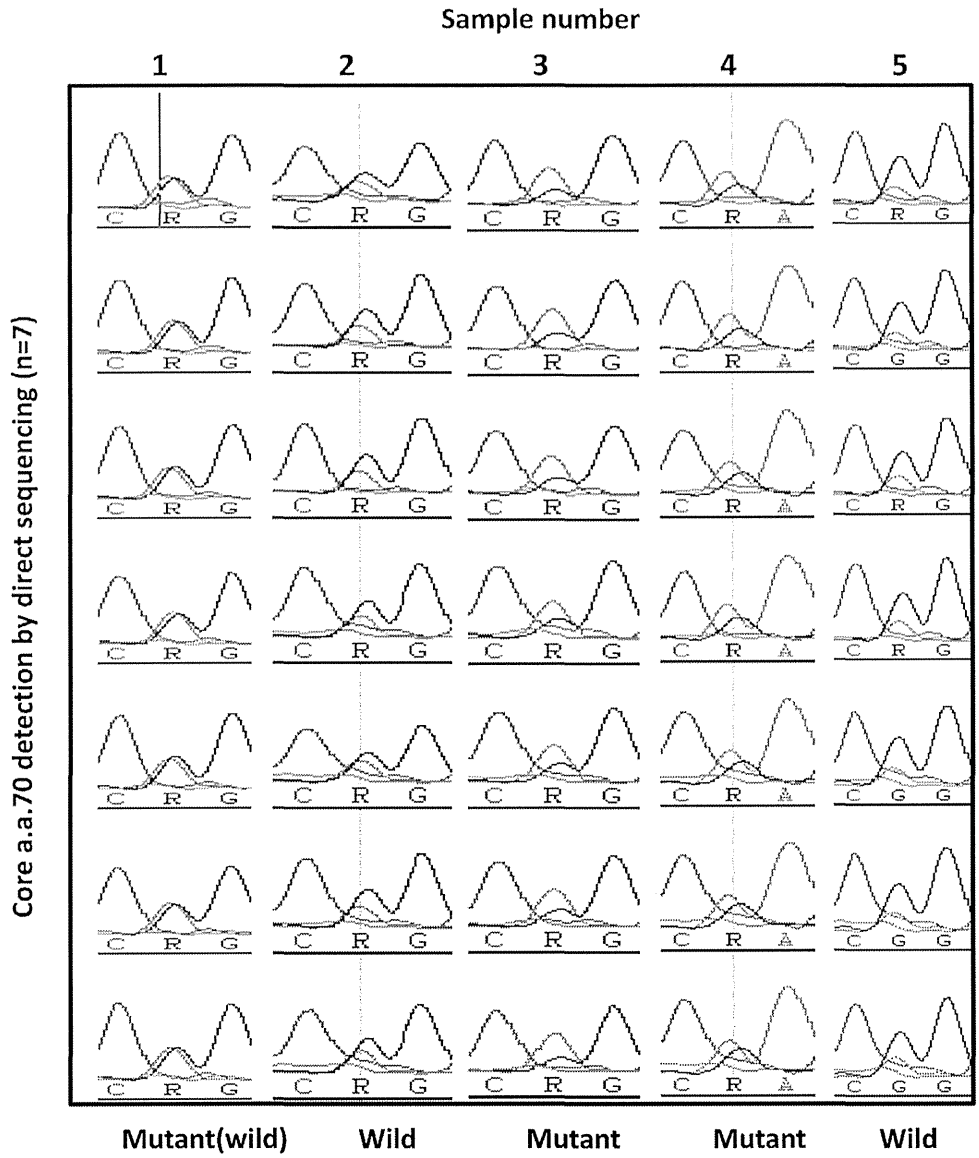

Fig. 1. The direct sequencing results are demonstrated by nucleotide sequence electropherograms. The HCV Core protein gene was amplified using nested PCR and sequenced using the BigDye Terminator v3.1 Cycle Sequencing Kit. Core a.a.70 substitutions were analyzed as described by Akuta et al. (2005). Samples from 87 patients were analyzed. The elution profiles for five samples indicated the presence of more than one sequence. Even after repeating the analysis seven times, the samples represented two mutant sequences and two wild-type sequences; however, it was difficult to distinguish whether sample 1 was mutant.

range of 0–100% of mutant plasmids mixed with wild-type plasmids (Pearson's $R^2 = 0.99$, $p < 0.0001$) (Fig. 3A). When the mutant and wild-type plasmids were mixed in various ratios, 0.005% of the mutants were detected (Fig. 3B) in the presence of 100,000 copies of wild-type plasmid DNA per assay. The assay was linear when the proportion of the mutant plasmid was 0.005%–10% of the entire plasmid population (Pearson's $R^2 = 0.999$, $p < 0.0001$, Fig. 3B). The mutant plasmid was undetectable when present as less than 0.0025% of the total DNA. The observed and expected results were correlated using HCV standard plasmids (1.25, 2.5, 5, 10, 100, 1000, 10,000, 100,000, 160,000, and 180,000 copies) (Fig. 3C and D). The ddPCR results agreed with the calculated values and were in accordance with acceptance of trueness. The dashed lines perpendicular to the *x*- and *y*-axes indicate concentrations below the limit of detection (LOD; 2.5 copies/well) and the highest number of copies (100,000) tested. Furthermore, the assay was linear (Pearson's $R^2 = 0.999$, $p < 0.0001$) above LOD.

3.5. Repeatability (intra-assay variation) and reproducibility (inter-assay variation) of ddPCR

The repeatability and reproducibility (Table 2) of the ddPCR assay was determined by performing replicate measurements of 12 different samples (genotype 1b; 0.05–99.88% mutant DNA). Intra- and inter-assay variabilities were assessed. Sufficient volume for three aliquots of each sample was stored at 4 °C until use. For each sample, three replicates were tested in the same assay to evaluate intra-assay repeatability. Inter-assay reproducibility was evaluated by testing two additional aliquots, each on a separate day. The intra-assay averages ± standard deviation (SD) of the log number of copies/mL of the mutant, wild type, mutant rare %, and accepted droplets, respectively, were as follows: 4.36 ± 0.03, 5.32 ± 0.03, 26.41 ± 0.09, and 13,008 ± 769. The inter-assay averages ± SD were as follows: 4.36 ± 0.03, 5.32 ± 0.04, 26.43 ± 0.14, and 11,725 ± 1908, respectively. These results also suggested that the repeatability (intra-assay) variability of the assay was good, as

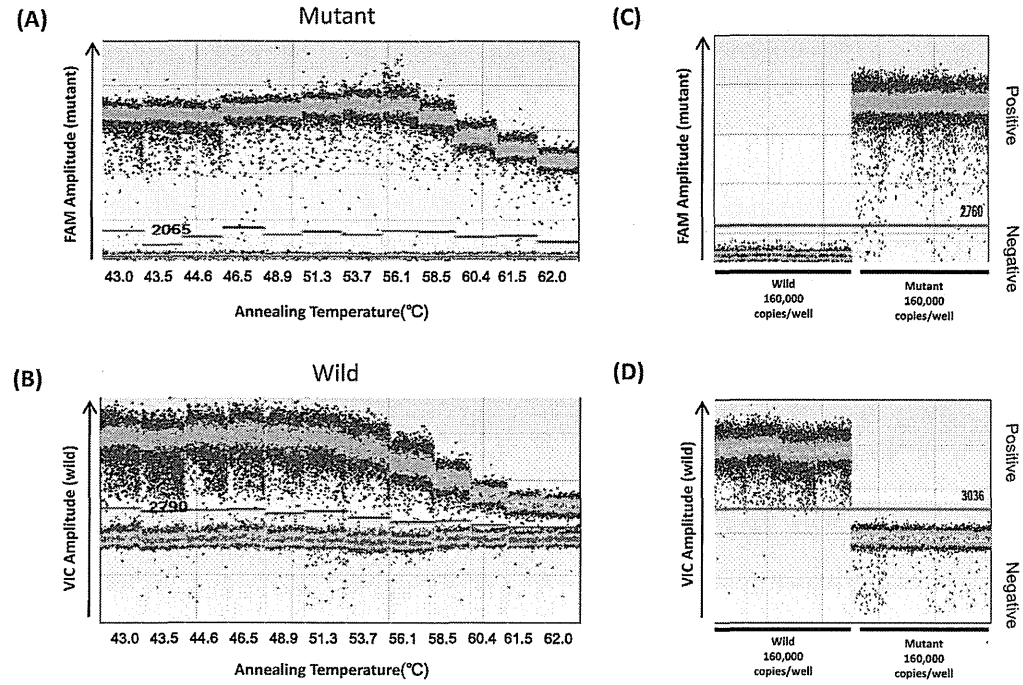

Fig. 2. Fluorescence amplitude plotted against annealing temperature. The assay was conducted across an annealing temperature gradient: 43.0, 43.5, 44.6, 46.5, 48.9, 51.3, 53.7, 56.1, 58.5, 60.4, 61.5, and 62.0 °C) (A and B). (A) FAM fluorescence amplitude of mutant plasmids (100,000 copies/well). (B) VIC fluorescence amplitude for wild-type plasmids (100,000 copies/well). (C) FAM fluorescence amplitude for mutant and wild-type plasmids (160,000 copies/each well). (D) VIC fluorescence amplitude for mutant and wild-type plasmids (160,000 copies/each well). The horizontal line indicates the threshold.

little variation was observed when samples were tested for reproducibility (inter-assay).

3.6. Correlation with the COBAS TaqMan® HCV RNA Test

The commercially available COBAS TaqMan® HCV RNA Test was used to confirm the accuracy of the quantitative results obtained using the ddPCR assay. The data generated by the analysis of clinical samples using the COBAS TaqMan® HCV Test were closely correlated with those of the ddPCR assay ($n = 87$, $p < 0.0001$, $y = 1.017x - 0.3111$, Pearson's $R^2 = 0.9120$, Fig. 4A). The arrows indicate a single point mutation, which was detected in 3 (3.45%) of the 87 samples (pattern 5, CTCGCCA*T*CCCGA; pattern 6, *Y*TCGCCGGCCCGA; and pattern7, CTCGCCG*T*CCCGA; Table 1). The data for the COBAS TaqMan® HCV Test and ddPCR assay were correlated for all samples, including each of the three samples. In addition, the results of quantitation of wild-type and mutant sequences obtained using ddPCR were compared with those obtained using the COBAS TaqMan® HCV Test. However, the data did not correlate for all quantified data of the mutant and wild-type sequences (Fig. 4B, $y = 0.4594x + 3.801$, Pearson's $R^2 = 0.4112$, $p < 0.0001$ and Fig. 4C, $y = 0.4584x + 4.076$, Pearson's $R^2 = 0.3673$, $p < 0.0001$, respectively). These data suggested that the novel assay could not only measure the frequency of mutations in Core a.a.70 but was also useful for the quantitation of mutations in the target gene in the polymorphic viral genome.

3.7. Correlation with direct sequencing

The results of ddPCR and direct sequencing were compared (Fig. 5). Direct nucleotide sequencing of the 87 patients with HCV infection was performed to determine mutation patterns in Core a.a.70. Wild-type and mutant sequences were found in 55 (63.2%) and 32 (36.8%) samples by direct sequencing, respectively. However, the ddPCR assay detected mutations in 85 (97.7%) of the 87 samples. The median frequencies were 0.262% ($n = 55$; range, 0–37.951%) and 99.687% ($n = 32$; range, 52.191–100%) for the wild-type and mutant sequences, respectively, by direct sequencing. These data indicated that mutations in Core a.a.70 existed in the wild-type sequences, although the frequencies were low.

3.8. Correlation with cloning

To address false positives, twenty clones in 32 clinical samples were picked up and analyzed the frequency of aa70 mutations by direct sequencing (Supplementary data 1). There are significantly correlated in the mutations between ddPCR and direct sequencing (Pearson's $R^2 = 0.975$, $p < 0.0001$). The three samples (nos. 1–3) showed less than 1% of the mutants by ddPCR. However, direct sequencing failed to detect mutant clones because of the differences in sensitivity and principles between the two methods. The error rates are thought to be reduced by removing the amplification efficiency reliance of qPCR and the data in Table 2 confirmed reproducibility. Further, no mutations were detected in HCV RNA negative samples from seven healthy patients (Supplementary data 2).

3.9. Validation analysis

Sixty-nine HCV-positive samples were prepared as validation sets. All mutations detected by direct sequencing were also detected by the ddPCR assay as first set measurements. To confirm whether the four patterns (nos. 1–4) of the seven probes in Table 1 were common among other HCV samples. The top 1–4 sequence patterns in Table 1 were found in 65 (94.2%) of the 69 patients. Therefore, the four sequences probes were common in HCV and sufficient to use for ddPCR (Supplementary data 3).

4. Discussion

In this paper, the development of a next-generation ddPCR assay for high-throughput, sensitive, and accurate quantitative

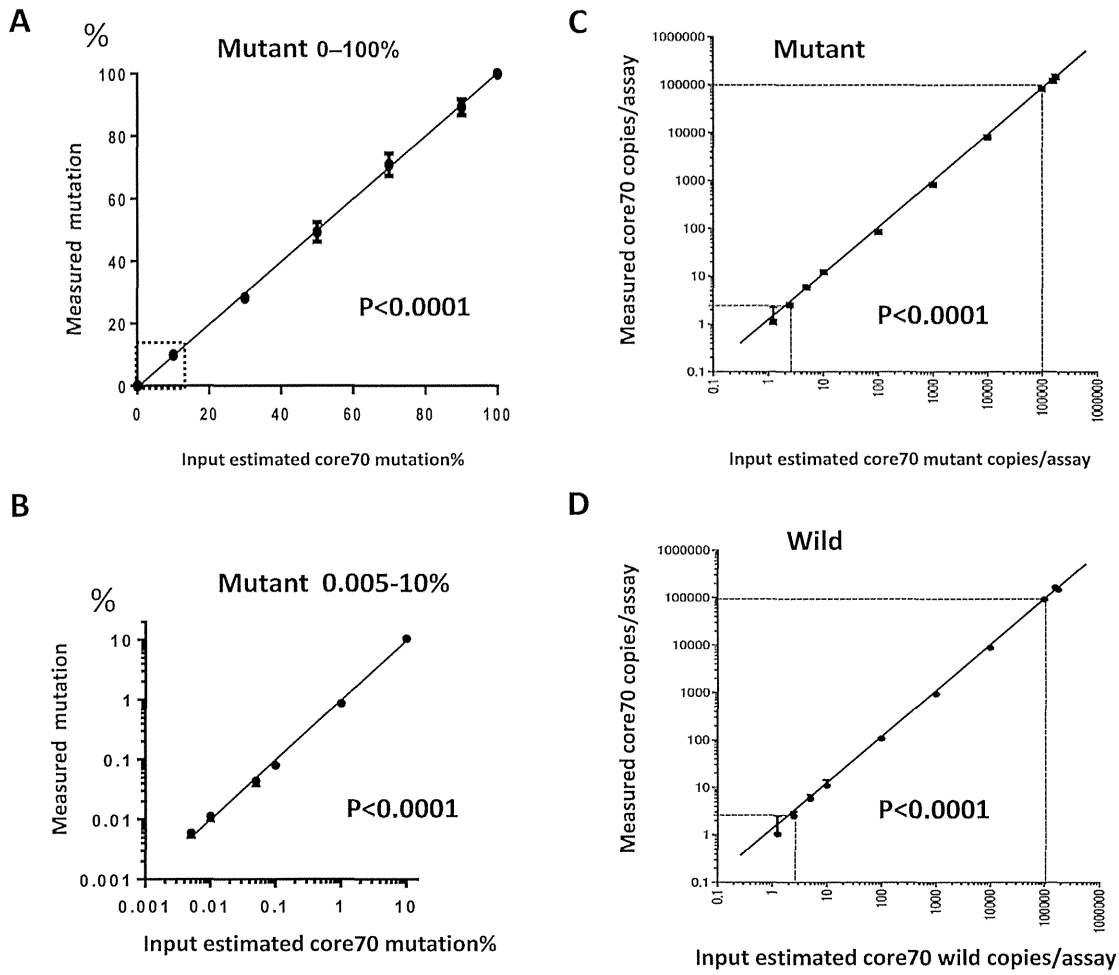

Fig. 3. Values are plotted against the estimated frequency (%) of the mutation in Core a.a.70. Error bars denote SD of the mutant ratio determined using ddPCR for each of five independent gravimetric dilutions. The number of plasmid DNA copies was 100,000 (A and B). (A) Plasmid DNA was mixed to 0, 10, 25, 50, 75, 90, and 100% of mutation (The square in A shows B). (B) Plasmid DNA was mixed so that the mutant sequence represented 0.0025%, 0.005%, 0.01%, 0.1%, 1.0%, and 10% of the population. The correlation between observed and expected results using HCV standard plasmids (1.25–180,000 copies/assay) was tested using the ddPCR assay (C and D). The dashed line indicates concentrations below LOD (2.5 copies/well) up to 100,000 copies (C and D). The assay was linear above LOD. (C) Mutant plasmid. (D) Wild-type plasmid.

detection of mutations in codon 70 of the HCV Core protein gene was described. This present study is the first to report that ddPCR is a powerful technique for the ultrasensitive and quantitative detection of single nucleotide polymorphisms within viral genomes. Furthermore, an important benefit of the ddPCR assay is that it can precisely quantitate the total amount of HCV RNA and determine whether mutations are present around the target point mutation of probes (Table 1, Fig. 4A).

The correlations between theoretical and experimental values were determined. To increase sensitivity and reproducibility, the novel assay employs a high-throughput automated instrument for preparing nucleic acids (Wenzel et al., 2010). Likewise, contamination, sensitivity, and reliability are key factors of any assay designed to detect mutations. The automated system incorporated an ultraviolet light decontamination system.

To clarify the effectiveness of the ddPCR assay, 87 clinical samples from patients with HCV infection were used for design purposes, and were analyzed for mutations in Core a.a.70 by direct sequencing and the ddPCR assay. All mutations detected by direct sequencing were also detected by the ddPCR assay. Moreover, the ddPCR assay detected mutant sequences present at extremely low frequencies. In particular, 32 (36.8%) of the 87 samples were identified as mutants for Core a.a. 70 by direct sequencing, while 85 (97.70%) of the 87 samples were identified as mutants by the ddPCR assay. Therefore, the ddPCR assay showed strong potential for highly precise quantitation of mutant HCV sequences in serum samples (CV%, intra-assay, 0.07–1.76; inter-assay, 0.04–1.76; Table 2). In intra- and inter-assays, CV% of a commercial HCV RNA quantitative assay (COBAS TaqMan®) ranged between 2.8% and 47.0% and 6.9–40.0%, respectively (Bossler et al., 2011). These results showed that the ddPCR assay is potentially more precise than the COBAS TaqMan® HCV Test, in accordance with the results of a recent report (Strain et al., 2013).

The HCV Core protein has oncogenic potential in transgenic mice and modifies the formation of reactive oxygen species (Korenaga et al., 2005; Moriya et al., 1998). Mutation in Core a.a.70 is an important primary factor that influences antiviral treatment efficacy, as well as the progression of liver disease and hepatocarcinogenesis (Okanoue et al., 2009; Akuta et al., 2012; Miura et al., 2013). However, the functional relevance of amino acid residue substitutions in the pathogenesis of hepatitis C is unknown. Therefore, it is important to develop more precise quantitative assays for the identification of mutants in order to understand the role of Core a.a.70. Currently available techniques, which are direct sequencing methods, are not sufficiently sensitive to detect mutations. Other methods, such as the TaqMan® amplification refractory mutation system and the Invader assay, have increased sensitivity to 1%. However, mutants are often present below this level, and LOD of

Table 2
Repeatability (intra-assay variation) and reproducibility (inter-assay variation) of ddPCR.

	No.	Mutant (log copies/mL)			Wild (log copies/mL)			Mutant (%)			Accepted droplets		
		Average	SD[1]	CV %[2]	Average	SD[1]	CV %[2]	Average	SD[1]	CV %[2]	Average	SD[1]	CV %[2]
Intra	1	3.53	0.06	1.76	6.92	0.01	0.16	0.05	0.01	13.02	14,167	866	6.11
	2	3.26	0.05	1.48	3.06	0.01	0.12	0.17	0.02	1051	1.1702	486	4.15
	3	3.04	0.01	0.47	5.34	0.01	0.09	0.27	0.01	4.39	14,049	1057	7.52
	4	3.53	0.05	1.59	5.75	0.07	1.27	0.59	0.02	3.89	14,064	501	3.53
	5	3.80	0.05	1.20	5.95	0.02	0.21	0.73	0.06	8.51	13,414	921	6.87
	5	3.90	0.01	0.35	5.81	0.16	6.06	1.32	0.03	2.80	13,644	1004	7.33
	7	4.71	0.02	0.49	8.08	0.01	0.21	4.42	0.22	5.32	12,776	481	3.76
	8	4.49	0.04	0.81	5.79	0.01	0.17	4.90	0.36	6.89	10,749	683	3.35
	9	4.69	0.01	0.16	5.94	0.01	0.12	5.65	0.11	1.73	13,792	925	6.70
	10	6.22	0.01	0.21	4.00	0.01	0.14	99.39	0.09	0.09	10,117	1209	11.95
	11	5.08	0.01	0.20	2.57	0.01	0.11	99.88	0.10	0.10	14,320	677	4.73
	12	6.02	0.00	0.07	3.38	0.05	1.47	9958	0.02	0.02	13,297	424	3.19
Total		4.36	0.03	0.73	5.32	0.03	0.84	26.41	0.09	4.78	13,008	769	6.02
Max		6.22	0.06	1.76	6.92	0.18	6.03	99.88	0.36	13.02	14,320	1209	11.95
Min		3.04	0.00	0.07	2.57	0.01	0.09	0.05	0.01	0.02	10,117	424	3.19
Inter	1	3.53	0.06	1.76	6.87	0.07	1.00	0.05	0.05	6.40	13,676	1820	13.30
	2	3.27	0.01	0.42	6.04	0.02	0.41	0.17	0.00	2.24	10,205	2116	20.74
	3	3.06	0.03	0.92	5.62	0.02	0.30	0.27	0.01	2.88	13,409	905	6.75
	4	3.52	0.02	0.70	5.75	0.02	0.26	0.59	0.01	1.95	12,041	2862	23.77
	5	3.81	0.02	0.60	5.92	0.04	0.60	0.80	0.09	11.90	12,157	1778	14.63
	6	3.87	0.04	111	5.79	0.03	0.54	1.18	0.20	16.74	11,509	3019	26.23
	7	4.71	0.00	0.04	6.07	0.02	0.37	4.28	0.22	5.27	10,263	3555	34.64
	8	4.51	0.03	0.71	5.78	0.01	0.15	5.08	0.26	5.21	9985	1081	10.83
	9	4.73	0.05	1.08	5.93	0.01	0.25	5.99	0.48	7.93	12,460	1884	15.12
	10	6.19	0.05	0.77	4.00	0.01	0.26	9955	0.06	0.06	9722	559	5.75
	11	5.09	0.01	0.18	2.62	0.08	3.09	99.65	0.07	0.07	13,258	1503	11.33
	12	6.06	0.06	1.04	3.50	0.21	5.88	99.70	0.17	0.17	12,013	1816	15.11
Total		4.36	0.03	0.78	5.32	0.04	1.09	26.42	0.14	5.05	11,725	1908	16.52
Max		6.19	0.06	1.76	6.87	0.21	5.88	99.70	0.48	16.74	13,373	3555	34.64
Min		3.06	0.00	0.04	2.32	0.01	0.15	0.05	0.00	0.06	9722	559	5.75

[1] Standard deviation.
[2] Coefficient of variation.

the ddPCR assay was 200-fold greater than that of the TaqMan® and Invader® assays (Nakamoto et al., 2009; Tadokoro et al., 2013). Another system, which was mutation-specific PCR, for detecting variants is not quantitative (Okamoto et al., 2007). Moreover, microfluidic chamber-based digital PCR was commercially available (Whale et al., 2013), however, it is expensive and the number of technical replicates that can be analyzed is limited.

UDPS techniques are prone to errors in base calling, alignment, and sequence data assembly (Nielsen et al., 2011). The error rate of UDPS techniques introduced by polymerase ranges from 0.01% to 1% (Noguchi et al., 2006), depending on the software used (Hoff, 2009), and UDPS has a higher error frequency than direct sequencing (Shendure and Ji, 2008). In addition, the sensitivity of the relative quantitative ddPCR assay was improved by 18.4-fold compared with a previously reported UDPS assay (Miura et al., 2013). Therefore, ddPCR was selected for the relative and absolute quantitative detection of mutations.

The ddPCR assay is ultrasensitive and offers high-throughput analysis, and therefore presents a potentially new assay to identify biomarkers of HCV-induced liver disease. Unfortunately, no report has yet provided statistical analysis of the relationship between the progression of liver disease and the rate of mutation in Core a.a.70. However, a new cut-off frequency of mutants to predict the prognosis of HCV-induced liver disease may be useful in future clinical studies.

The results of this study indicated that the ddPCR assay can be used for analysis of HCV mutations, although total quantitation of hepatitis viral sequences has not been reported. In general, the ddPCR assay performed well to identify single nucleotide polymorphisms in the human genome. The mutation rate of RNA viruses is higher than that of human genome (Holland et al., 1982). The ddPCR assay was thought to be unsuitable for the quantitation of

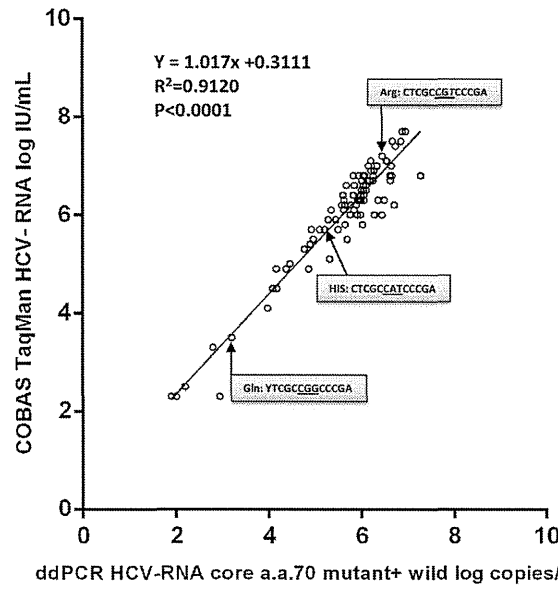

Fig. 4. Correlation between the results of 87 clinical specimens analyzed using the COBAS TaqMan® HCV Test and ddPCR assay combined with sample processing using a MagNA Pure LC instrument ($y = 1.017x + 0.3111$, Pearson's $R^2 = 0.9120$, $p < 0.0001$). Arrows point to the correlation of the results of the COBAS TaqMan® Test and ddPCR assay of three samples with a single point mutation complementary to the probe. The italic letters of nucleic acid sequence show the mutations and the underlines indicate at the codon of Core a.a. Total HCV RNA (mutant + wild-type copies/mL) was determined using the ddPCR assay (horizontal line) and COBAS TaqMan® HCV Test (vertical line).

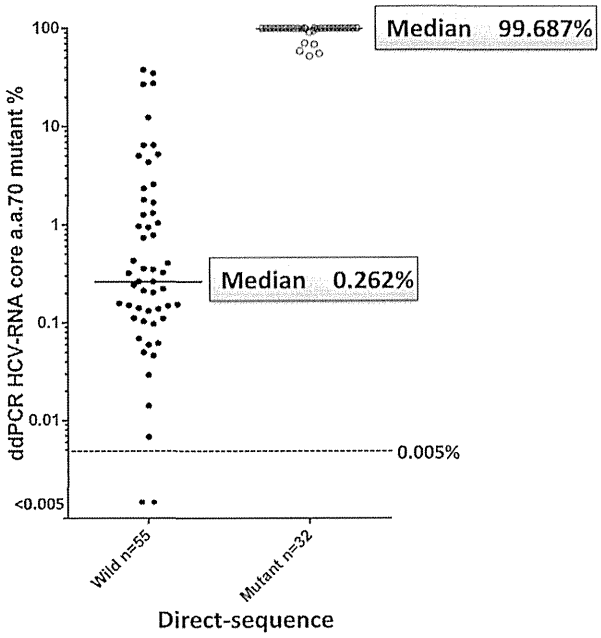

Fig. 5. Comparison between the results of 87 clinical specimens analyzed by direct sequencing and the ddPCR assay. The ddPCR assay detected all of the mutations that were detected by direct sequencing (wild type: $n = 55$; median, 0.262%; range, 0–37.951%; mutant: $n = 32$; median, 99.687%; range, 52.191–100%).

single mutations within a highly polymorphic genome, such as HCV and HIV because many variants in near target sequences and setting probes affected quantitation. However, Strain et al. (2013) reported that ddPCR could be used for the quantitation of HIV. In addition, there were fewer mutations in near Core a.a. 70. These data suggest that ddPCR technology is useful for the quantitation of mutations in other viruses with highly polymorphic genomes, if there are few variant sequences in near targets.

Therefore, it was hoped that this new assay could be used for the quantitation of mutations in other viral genomes, such as of mutations in HCV resistant to direct-acting antivirals (Aloia et al., 2012; Wong et al., 2013; Conteduca et al., 2014), mutations in drug-resistant HBV (Mukaide et al., 2010), and mutations associated with HBV reactivation (Dai et al., 2001; Alexopoulou et al., 2006) in patients receiving chemotherapy.

5. Conclusions

A novel, high-throughput and ultrasensitive assay was developed to quantitate mutations in HCV codon a.a.70. Therefore, ddPCR technology should be useful for the relative and absolute quantitation of HCV mutations as well as mutations in the polymorphic genomes of other viruses.

Acknowledgments

This work was supported by a grant (22-108, 25-202) from the National Center for Global Health and Medicine in Japan and in part by the Japanese Ministry of Health, Labor and Welfare grant (H23-007) and the Japanese Ministry of Education, Culture, Sports, and Science (No. 22590750). The authors thank Bio-Rad Laboratories KK, Japan (Mr. Hiroto Tsuruta, Ms. Issei Iijima, Mr. Tsutomu Daito, Mr. Yukinori Yatsuda, and Mr. Keisuke Uchida) for their professional opinions and technical support. The authors thank Mr. Makoto Yamashiro (Roche Diagnostics KK Japan) for his professional opinions and technical support. The authors thank all of the members of our laboratory (Ms. Yoko Tamada, Ms. Sachiko Sato, Ms. Miki Yoshida, Ms. Mami Ohashi, Ms. Ayano Ito, Mr. Hideyuki Aoshima, Mr. Takashi Tsunoda, Ms. Hiroko Higashimoto, Mr. Youji Hirabayashi, Mr. Akio Ueda, and Mr. Isao Tada).

Appendix A. Supplementary data

Supplementary material related to this article can be found, in the online version, at http://dx.doi.org/10.1016/j.jviromet.2014.07.006.

References

Akuta, N., Suzuki, F., Seko, Y., Kawamura, Y., Sezaki, H., Suzuki, Y., Hosaka, T., Kobayashi, M., Hara, T., Kobayashi, M., Saitoh, S., Arase, Y., Ikeda, K., Kumada, H., 2012. Complicated relationships of amino acid substitution in hepatitis C virus core region and IL28B genotype influencing hepatocarcinogenesis. Hepatology 56, 2134–2141.

Akuta, N., Suzuki, F., Sezaki, H., Suzuki, Y., Hosaka, T., Someya, T., Kobayashi, M., Saitoh, S., Watahiki, S., Sato, J., Matsuda, M., Kobayashi, M., Arase, Y., Ikeda, K., Kumada, H., 2005. Association of amino acid substitution pattern in core protein of hepatitis C virus genotype 1b high viral load and non-virological response to interferon-ribavirin combination therapy. Intervirology 48, 372–380.

Alexopoulou, A., Theodorou, M., Dourakis, S.P., Karayiannis, P., Sagkana, E., Papanikolopoulos, K., Archimandritis, A.J., 2006. Heparitis B virus reactivation in patients receiving chemotherapy for malignancies: role of precore stop-codon and basic core promoter mutations. J. Viral. Hepat. 13, 591–596.

Aloia, A.L., Locarnini, S., Beard, M.R., 2012. Antiviral resistance and direct-acting antiviral agents for HCV. Antivir. Ther. 17, 1147–1162.

Becker-andr, M., Hahlbrock, K., 1989. Absolute mRNA quantification using the polymerase chain reaction (PCR). A novel approach by a PCR aided transcript titration assay (PATITY). Nucleic Acids Res., 9437–9446.

Bossler, A., Gunsolly, C., Pyne, M.T., Rendo, A., Rachel, J., Mills, R., Miller, M., Sipley, J., Hillyard, D., Jenkins, S., Essmyer, C., Young, S., Lewinski, M., Rennert, H., 2011. Performance of the COBAS® AmpliPrep/COBAS TaqMan® automated system for hepatitis C virus (HCV) quantification in a multi-center comparison. J. Clin. Virol. 50, 100–103 (the official publication of the Pan American Society for Clinical Virology).

Conteduca, V., Sansonno, D., Russi, S., Pavone, F., Dammacco, F., 2014. Therapy of chronic heparitis C virus infection in the era of direct-acting and host-targeting antiviral agents. J. Infect. 68, 1–20.

Dai, M.S., Lu, J.J., Chen, Y.C., Perng, C.L., Chao, T.Y., 2001. Reactivation of precore mutant hepatitis B virus in chemotherapy-treated patients. Cancer 92, 2927–2932.

Edelmann, a., Eichenlaub, U., Lepek, S., Krüger, D.H., Hofmann, J., 2013. Performance of the MagNA Pure 96 system for cytomegalovirus nucleic acid amplification testing in clinical samples. J. Clin. Microbiol. 51, 1600–1601.

Gilliland, G., Perrin, S., Blanchard, K., Bunn, H.F., 1990. Analysis of cytokine mRNA and DNA: detection and quantitation by competitive polymerase chain reaction. Proc. Nat. Acad. Sci. U.S.A. 87, 2725–2729.

Glenn, T.C., 2011. Field guide to next-generation DNA sequencers. Mol. Ecol. Res. 11, 759–769.

Grakoui, A., Wychowski, C., Lin, C., Feinstone, S.M., Rice, C.M., 1993. Expression and identification of hepatitis C virus polyprotein cleavage products. J. Virol. 67, 1385–1395.

Higuchi, R., Fockler, C., Dollinger, G., Watson, R., 1993. Kinetic PCR analysis: real-time monitoring of DNA amplification reactions. Biotechnology 11, 1026–1030.

Hindson, B.J., Ness, K.D., Masquelier, D.a, Belgrader, P., Heredia, N.J., Makarewicz, A.J., Bright, I.J., Lucero, M.Y., Hiddessen, A.L., Legler, T.C., Kitano, T.K., Hodel, M.R., Petersen, J.F., Wyatt, P.W., Steenblock, E.R., Shah, P.H., Bousse, L.J., Troup, C.B., Mellen, J.C., Wittmann, D.K., Erndt, N.G., Cauley, T.H., Koehler, R.T., So, A.P., Dube, S., Rose, K.a, Montesclaros, L., Wang, S., Stumbo, D.P., Hodges, S.P., Romine, S., Milanovich, F.P., White, H.E., Regan, J.F., Karlin-Neumann, G.a, Hindson, C.M., Saxonov, S., Colston, B.W., 2011. High-throughput droplet digital PCR system for absolute quantitation of DNA copy number. Anal. Chem. 83, 8604–8610.

Hoff, K.J., 2009. The effect of sequencing errors on metagenomic gene prediction. BMC Genom. 10, 520.

Holland, J., Spindler, K., Horodyski, F., Grabau, E., Nichol, S., VandePol, S., 1982. Rapid evolution of RNA genomes. Science 215, 1577–1585.

Hubers, a.J., Heideman, D.aM., Yatabe, Y., Wood, M.D., Tull, J., Tarón, M., Molina, M.a, Mayo, C., Bertran-Alamillo, J., Herder, G.J.M., Koning, R., Sie, D., Ylstra, B., Meijer, G.a, Snijders, P.J.F., Witte, B.I., Postmus, P.E., Smit, E.F., Thunnissen, E., 2013. EGFR mutation analysis in sputum of lung cancer patients: a multitechnique study. Lung Cancer 82, 38–43.

Kiyosawa, K., Sodeyama, T., Tanaka, E., Gibo, Y., Yoshizawa, K., Nakano, Y., Furuta, S., Akahane, Y., Nishioka, K., Purcell, R.H., 1990. Interrelationship of blood transfusion, non-A, non-B hepatitis and hepatocellular carcinoma: analysis by detection of antibody to hepatitis C virus. Hepatology 12, 671–675.

Korenaga, M., Wang, T., Li, Y., Showalter, L.a, Chan, T., Sun, J., Weinman, S.a, 2005. Hepatitis C virus core protein inhibits mitochondrial electron transport and increases reactive oxygen species (ROS) production. J. Biol. Chem. 280, 37481–37488.

Liang, T.J., Rehermann, B., Seeff, L.B., Hoofnagle, J.H., 2000. Pathogenesis, natural history, treatment, and prevention of hepatitis C. Ann. Intern. Med. 132, 296–305.
Miura, M., Maekawa, S., Kadokura, M., Sueki, R., Komase, K., Shindo, H., Ohmori, T., Kanayama, A., Shindo, K., Amemiya, F., Nakayama, Y., Kitamura, T., Uetake, T., Inoue, T., Sakamoto, M., Okada, S., Enomoto, N., 2011. Analysis of viral amino acids sequences and the IL28B SNP influencing the development of hepatocellular carcinoma in chronic hepatitis C. Hepatol. Int., 386–396.
Miura, M., Maekawa, S., Takano, S., Komatsu, N., Tatsumi, A., Asakawa, Y., Shindo, K., Amemiya, F., Nakayama, Y., Inoue, T., Sakamoto, M., Yamashita, A., Moriishi, K., Enomoto, N., 2013. Deep-sequencing analysis of the association between the quasispecies nature of the hepatitis C virus core region and disease progression. J. Virol. 87, 12541–12551.
Morisset, D., Štebih, D., Milavec, M., Gruden, K., Žel, J., 2013. Quantitative analysis of food and feed samples with droplet digital PCR. PLoS One 8, e62583.
Moriya, K., Fujie, H., Shintani, Y., Yotsuyanagi, H., Tsutsumi, T., Ishibashi, K., Matsuura, Y., Kimura, S., Miyamura, T., Koike, K., 1998. The core protein of hepatitis C virus induces hepatocellular carcinoma in transgenic mice. Nat. Med. 4, 1065–1067.
Mukaide, M., Tanaka, Y., Shin-I, T., Yuen, M.-F., Kurbanov, F., Yokosuka, O., Sata, M., Karino, Y., Yamada, G., Sakaguchi, K., Orito, E., Inoue, M., Baqai, S., Lai, C.-L., Mizokami, M., 2010. Mechanism of entecavir resistance of hepatitis B virus with viral breakthrough as determined by long-term clinical assessment and molecular docking simulation. Antimicrob. Agents Chemother. 54, 882–889.
Nakamoto, S., Kanda, T., Yonemitsu, Y., Arai, M., Fujiwara, K., Fukai, K., Kanai, F., Imazeki, F., Yokosuka, O., 2009. Quantification of hepatitis C amino acid substitutions 70 and 91 in the core coding region by real-time amplification refractory mutation system reverse transcription-polymerase chain reaction. Scand. J. Gastroenterol. 44, 872–877.
Niederau, C., Lange, S., Heintges, T., Erhardt, A., Buschkamp, M., Hürter, D., Nawrocki, M., Kruska, L., Hensel, F., Petry, W., Häussinger, D., 1998. Prognosis of chronic hepatitis C: results of a large, prospective cohort study. Hepatology 28, 1687–1695.
Nielsen, R., Paul, J.S., Albrechtsen, A., Song, Y.S., 2011. Genotype and SNP calling from next-generation sequencing data. Nat. Rev. Genet. 12, 443–451.
Noguchi, H., Park, J., Takagi, T., 2006. MetaGene: prokaryotic gene finding from environmental genome shotgun sequences. Nucleic Acids Res. 34, 5623–5630.
Okamoto, K., Akuta, N., Kumada, H., Kobayashi, M., Matsuo, Y., Tazawa, H., 2007. A nucleotide sequence variation detection system for the core region of hepatitis C virus-1b. J. Virol. Methods 141, 1–6.
Okanoue, T., Itoh, Y., Hashimoto, H., Yasui, K., Minami, M., Takehara, T., Tanaka, E., Onji, M., Toyota, J., Chayama, K., Yoshioka, K., Izumi, N., Akuta, N., Kumada, H., 2009. Predictive values of amino acid sequences of the core and NS5A regions in antiviral therapy for hepatitis C: a Japanese multi-center study. J. Gastroenterol. 44, 952–963.
Pekin, D., Skhiri, Y., Baret, J.-C., Le Corre, D., Mazutis, L., Salem, C., Ben Millot, F., El Harrak, A., Hutchison, J.B., Larson, J.W., Link, D.R., Laurent-Puig, P., Griffiths, A.D., Taly, V., 2011. Quantitative and sensitive detection of rare mutations using droplet-based microfluidics. Lab Chip 11, 2156–2166.
Pinheiro, L.B., Coleman, V.A., Hindson, C.M., Herrmann, J., Hindson, B.J., Bhat, S., Emslie, K.R., 2012. Evaluation of a droplet digital polymerase chain reaction format for DNA copy number quantification. Anal. Chem. 84, 1003–1011.
Porcher, C., Malinge, M.C., Picat, C., Grandchamp, B., 1992. A simplified method for determination of specific DNA or RNA copy number using quantitative PCR and an automatic DNA sequencer. BioTechniques 13, 106–114.
Roche-PCR-Chapters, 2009. PCR Applications Manual, Chapters 2, General Guidelines. Roche-PCR-Chapters.
Shendure, J., Ji, H., 2008. Next-generation DNA sequencing. Nat. Biotechnol. 26, 1135–1145.
Strain, M.C., Lada, S.M., Luong, T., Rought, S.E., Gianella, S., Terry, V.H., Spina, C.a, Woelk, C.H., Richman, D.D., 2013. Highly precise measurement of HIV DNA by droplet digital PCR. PLoS One 8, e55943.
Syvänen, A.C., Bengtström, M., Tenhunen, J., Söderlund, H., 1988. Quantification of polymerase chain reaction products by affinity-based hybrid collection. Nucleic Acids Res. 16, 11327–11338.
Tadokoro, K., Kobayashi, M., Suzuki, F., Tanaka, C., Yamaguchi, T., Nagano, M., Egashira, T., Kumada, H., 2013. Comparative quantitative analysis of hepatitis C mutations at amino acids 70 and 91 in the core region by the Q-Invader assay. J. Virol. Methods 189, 221–227.
Thermo Scientific, 2013. DNA Copy Number Calculater. Thermo Scientific. http://www.thermoscientificbio.com/EktronTemplates/FullContent.aspx?id=17179928879&rdr=true&LangType=1041 (accessed 08.11.13).
Thomas, D.L., 2013. Global control of hepatitis C: where challenge meets opportunity. Nat. Med. 19, 850–858.
Vogelstein, B., Kinzler, K.W., 1999. Digital PCR. Proc. Nat. Acad. Sci. U.S.A. 96, 9236–9241.
Wenzel, J.J., Panning, M., Kaul, K.L., Mangold, K.a, Revell, P.a, Luna, R.A., Zepeda, H., Perea, L., Vazquez-Perez, J.a, Young, S., Rodic-Polic, B., Eickmann, M., Drosten, C., Jilg, W., Reischl, U., 2010. Analytical performance determination and clinical validation of the novel Roche RealTime Ready Influenza A/H1N1 Detection Set. J. Clin. Microbiol. 48, 3088–3094.
Whale, A.S., Cowen, S., Foy, C.A., Huggett, J.F., 2013. Methods for applying accurate digital PCR analysis on low copy DNA samples. PLoS One 8, e58177.
Wong, K.A., Worth, A., Martin, R., Svarovskaia, E., Brainard, D.M., Lawitz, E., Miller, M.D., Mo, H., 2013. Characterization of hepatitis C virus resistance from a multiple-dose clinical trial of the novel NS5A inhibitor GS-5885. Antimicrob. Agents Chemother. 57, 6333–6340.
Yang, J.D., Roberts, L.R., 2010. Hepatocellular carcinoma: a global view. Nat. Rev. Gastroenterol. Hepatol. 7, 448–458.

Journal of Medical Virology 86:241–247 (2014)

Significance of Liver Stiffness Measurement by Acoustic Radiation Force Impulse (ARFI) Among Hepatitis C Patients

Ryoko Yamada,[1] Naoki Hiramatsu,[1]* Tsugiko Oze,[1] Naoki Morishita,[1] Naoki Harada,[1] Masanori Miyazaki,[1] Takayuki Yakushijin,[1] Takuya Miyagi,[1] Yuichi Yoshida,[1] Tomohide Tatsumi,[1] Tatsuya Kanto,[1] Norio Hayashi,[2] and Tetsuo Takehara[1]

[1]*Department of Gastroenterology and Hepatology, Osaka University Graduate School of Medicine, Suita City, Osaka, Japan*

[2]*Kansai Rousai Hospital, Amagasaki, Hyogo, Amagasaki City, Hyougo, Japan*

The degree of liver fibrosis is strongly associated with the antiviral effect of interferon on chronic hepatitis C patients. In this study, the accuracy of acoustic radiation force impulse (ARFI) in assessing liver fibrosis and the association between liver stiffness using ARFI and antiviral effects were investigated. The 124 patients with chronic hepatitis C enrolled in this study included 94 with HCV genotype 1 and 40 (30%) with moderate fibrosis (METAVIR fibrosis score $\geq$F2). Sixty-one patients received pegylated interferon (peg-IFN) plus ribavirin combination therapy and the treatment responses were assessed. The shear wave velocity (Vs value) by ARFI had a strong correlation with the histological fibrosis stage ($P<0.001$). The AUROC of the Vs value, aspartate aminotransferase platelet ratio index and FIB4 for the diagnoses of moderate fibrosis ($\geq$F2) were 0.890, 0.779, and 0.737, respectively. HCV genotype 1 patients with the TT allele of IL28B and with a low Vs value (<1.40 m/sec) who were treated with peg-IFN plus ribavirin therapy achieved a sustained virologic response at a rate of 79% (15/19), while all patients with the TG/GG allele of IL28B and a high Vs value ($\geq$1.40 m/sec) experienced a non-virologic response (6/6). The Vs value measured by ARFI could not predict the treatment response for patients with HCV genotype 2. It is concluded that the combination of ARFI at cut off of 1.4 m/sec and IL28B may be useful for patients with chronic hepatitis C with genotype 1 treated with peg-IFN/ribavirin combination therapy. ***J. Med. Virol. 86:241–247, 2014.***

KEY WORDS: chronic hepatitis C; pegylated interferon plus ribavirin combination therapy; liver fibrosis; IL28B

INTRODUCTION

Interferon (IFN) is capable of eradicating hepatitis C virus and suppressing the progression of liver fibrosis and incidence of hepatocellular carcinoma, thus leading to a better prognosis [Hiramatsu et al., 1995; Kasahara et al., 1998, 2004; Manns et al., 2001; Fried et al., 2002; Hadziyannis et al., 2004; Kurokawa et al., 2009]. On the other hand, the progression of liver fibrosis has been indicated to be an important predictive factor for the treatment response to pegylated interferon (peg-IFN) plus ribavirin combination therapy for chronic hepatitis C [Hadziyannis et al., 2004; Everson et al., 2006; Oze et al., 2011]. Generally, the degree of liver fibrosis is classified histologically into stages according to the METAVIR and Ishak scoring systems [Ishak et al., 1995; Bedossa and Poynard, 1996]. Although liver biopsy has remained the gold standard for the most

Grant sponsor: Merck Sharp & Dohme; Grant sponsor: Chugai Pharmaceutical

Disclosures: Professor Tetsuo Takehara received scholarship funds from Merck Sharp & Dohme and Chugai Pharmaceutical. Dr. Tatsuya Kanto has an affiliation with a department funded by donations from Merck Sharp & Dohme.

*Correspondence to: Naoki Hiramatsu, MD, PhD, Department of Gastroenterology and Hepatology, Osaka University Graduate School of Medicine, 2-2, Yamadaoka, Suita City, Osaka 565-0871, Japan. E-mail: hiramatsu@gh.med.osaka-u.ac.jp

Accepted 6 October 2013

DOI 10.1002/jmv.23840

Published online 5 November 2013 in Wiley Online Library (wileyonlinelibrary.com).

accurate assessment of liver fibrosis, this invasive procedure has its limitations. Biopsies can cause bleeding, pain, and anxiety, and it is thus difficult to perform repeatedly. Non-invasive methods for the assessment of liver fibrosis include biochemical markers, such as hyaluronic acid and type 4 collagen 7S, liver fibrosis formulae combined with hematological and biochemical markers, such as aspartate aminotransferase platelet ratio index (APRI) and FIB4, and ultrasonic diagnostic methods, such as Fibroscan® (Echosens, Paris, France) and shear wave elastography [Wai et al., 2003; Sterling et al., 2006; Degos et al., 2010]. Recently, acoustic radiation force impulse (ARFI) (Siemens Medical Solutions, Mountain View, CA) has been developed in clinical practice as a non-invasive modality for assessing liver fibrosis [Friedrich-Rust et al., 2009; Toshima et al., 2011]. However, it is not clear whether Vs values by ARFI can be utilized as predictive factors for the treatment response to peg-IFN plus ribavirin combination therapy. It is also not clear whether ARFI and IL28B (rs8099917), which has been known to have a great impact on treatment response in genotype 1 patients, have an effect on each other in the prediction of treatment response [Tanaka et al., 2009].

The present study investigated the accuracy of ARFI in assessing liver fibrosis and its usefulness for predicting the treatment response to peg-IFN plus ribavirin combination therapy in patients with chronic hepatitis C.

PATIENTS AND METHOD

A total of 124 patients with chronic hepatitis C who were admitted to Osaka University Hospital between August 2009 and May 2012 were enrolled in this study. The eligibility criteria for this study required that the patients did not have decompensated cirrhosis or other forms of liver disease (e.g., alcohol liver disease, autoimmune hepatitis) or coinfection with hepatitis B or human immunodeficiency virus. Vs values were measured by ARFI at the start of treatment. Liver fibrosis was assessed histologically by liver biopsy for all patients, and every ARFI measurement was performed within 1 week preceding liver biopsy. The histological assessment of liver fibrosis was ranked from F0 to F4 based on the METAVIR scoring system. The study was conducted in accordance with the Declaration of Helsinki, as amended in 2002. Informed consent was obtained from all study participants.

Of the 124 patients, 68 received peg-IFN plus ribavirin combination therapy. All patients received peg-IFN alfa-2a (Pegasys; Roche, Basel, Switzerland) plus ribavirin (Copegus; Roche), or peg-IFN alfa-2b (Pegintron; Merck Whitehouse Station, NJ) plus ribavirin (Rebetol; Merck). The administration dose was set as follows: peg-IFN alfa-2a, 180 μg/week; peg-IFN alfa-2b, 1.5 μg/kg/week; ribavirin, body weight ≤60 kg, 600 mg/day; 60–80 kg, 800 mg/day; >80 kg, 1,000 mg/day. Of the 68 patients, 6 patients discontinued treatment because of adverse effects, and 1 patient was missing. A total of 61 patients, including 46 with HCV genotype 1 and 15 with genotype 2, completed the treatment.

The serum HCV RNA levels were analyzed qualitatively using the COBAS TaqMan HCV test (lower limit of detection 1.2–7.8 log IU/ml; Roche Diagnostics, Branchburg, NJ). The serum HCV RNA level for each patient with genotype 1 was measured at baseline, weeks 4, 12, 24, 36, 48, end of treatment and week 24 after the treatment. For genotype 2 patients, the HCV RNA levels were measured at baseline, weeks 4, 12, 24, and week 24 after the treatment. In patients with HCV genotype 1, a virologic response was defined as an undetectable serum HCV RNA level within 24 weeks, and all other responses were defined as non-virologic responses. A rapid virologic response was defined as an undetectable serum HCV RNA level at week 4, a complete early virologic response was defined as an undetectable serum HCV RNA level at week 12, and a late virologic response was defined as a detectable serum HCV RNA level at week 12 and an undetectable level at week 24. A sustained virologic response was defined as an undetectable serum HCV RNA level at week 24 after the treatment.

The treatment protocol defined duration as 48–72 weeks for genotype 1 patients, according to response-guided therapy; patients with a complete early virologic response received treatment for up to 48 weeks, and those with a late virologic response received treatment for up to 72 weeks. As a result, 17 patients with genotype 1 received treatment for 72 weeks. All of the genotype 2 patients were treated for 24 weeks.

IL28B Genotyping

Human genomic DNA was extracted from a whole blood sample of each patient. Single nucleotide polymorphisms (SNPs) located near the interleukin 28B (IL28B) gene (rs8099917) were determined using a real-time PCR system. Each extracted DNA was used for PCR with primers and probes from a commercial kit (Taqman SNP Genotyping Assays, Applied Biosystems, Foster City, CA). The SNP of IL28B was amplified, and the results were analyzed by real-time PCR in a thermal cycler (7900 Real-time PCR System, Applied Biosystems). Because patients with a homozygous TT genotype at this locus had significantly higher rates of a sustained virologic response than those who carried the G allele, the patients were stratified into two groups according to whether they had the TT allele or the TG/GG allele of the IL28B genotype.

ARFI Imaging

Liver stiffness was evaluated using Acuson S2000 within 1 month before the start of treatment. In this evaluation, an ARFI is followed by detection pulses to calculate the Vs value. Tracking beams that are

sensitive to more than 1/100 the wavelength of sound are applied adjacent to the push pulse. The time between the generation of the shear wave and the passing of the shear wave peak at an adjacent location is utilized to compute the shear wave velocity. The degree of tissue stiffness is quantified by shear wave speed, Vs (m/sec), which increases with tissue stiffness. The shear wave velocity is measured within a defined region of interest (ROI) (a central window of 5 mm axial × 4 mm width). In the actual examination, the ROI was located in an area without large blood vessels or bile ducts in the right lobe of the liver, through the intercostal space and at a depth of approximately 2 cm below the liver capsule. The mean value of shear wave velocity calculated from 10 measurements was defined as the Vs value.

Predictive Formulae of Liver Fibrosis

APRI and FIB4, which are existing formulae for predicting the progression of liver fibrosis, were used as a non-invasive method to measure liver fibrosis. They are defined as follows:

$$\text{APRI} = \text{AST(/ULN)} \times 100/\text{platelet}\,(\times 10^9/\text{L})$$

$$\text{FIB4} = \text{age} \times \text{AST}/(\text{platelet count}\,[\times 10^9/\text{L}] \times \text{ALT}^{1/2})$$

Statistical Analysis

The baseline continuous variables were expressed as the means ± standard deviation, and categorical variables were expressed as frequencies. The Pearson product–moment correlation coefficient was used to assess the correlation between two variables. The diagnostic accuracies of the non-invasive tests were estimated by comparison with the histological fibrosis stage, which was assessed using the METAVIR scoring system. The diagnostic performance of ARFI and serum fibrosis markers for liver fibrosis was assessed using receiver operating characteristic (ROC) curves. The ROC curve represented sensitivity versus (1—specificity) for all possible cut off values for predicting the different fibrosis stages. The areas under the curve (AUCs) and the 95% confidence intervals of the AUC values were calculated. The difference between the AUCs was tested by the DeLong test. A paired *t*-test was used to analyze the differences between continuous variables before and after the treatment. Univariate and multivariate logistic regression analyses were performed to identify the factors associated with a sustained virologic response. A P-value <0.05 was considered significant. Statistical analysis was conducted using SPSS version 17.0J (IBM, Armonk, NY) and MedCalc vesion12 software (MedCalc, Mariakerke, Belgium).

RESULTS

Baseline Characteristics of Patients

The overall study population of 124 patients consisted of 56 males (45%) and 94 patients (76%) infected with HCV genotype 1 (Table I). The mean age was 57.0 ± 12.1 years, and the mean body mass index (BMI) value was 22.6 ± 3.0 kg/m^2. The distribution of METAVIR fibrosis scores, F1, F2, F3, F4 was 84 (68%), 14 (11%), 14 (11%), and 12 (10%), respectively. The mean Vs value according to ARFI measurements was 1.39 ± 0.52 m/sec.

TABLE I. Characteristics of Enrolled Patients

		Treated patients (n = 61)	
	All patients (n = 124)	Genotype 1 (n = 46)	Genotype 2 (n = 15)
Gender (male/female)	56/68	17/29	7/8
Age (year)	57.0 ± 12.1	57.0 ± 11.8	52.1 ± 16.5
BMI (kg/m^2)	22.6 ± 3.0	22.5 ± 3.6	22.9 ± 3.4
Previous IFN treatment (naïve/experienced)	75/47	34/12	12/3
IL28B SNP (rs8099917) (TT/TG/GG)	79/25/2	32/11/2	12/1/0
Liver histology: activity (A0/A1/A2/A3)	0/115/7/1	0/43/2/1	0/14/1/0
Liver histology: fibrosis (F0/F1/F2/F3/F4)	0/84/14/14/11	0/28/8/5/5	0/11/3/1/0
HCV-RNA (log IU/ml)	6.20 ± 0.97	6.31 ± 0.82	6.08 ± 0.65
Platelet (×10^4/μl)	16.61 ± 5.10	16.14 ± 4.61	16.88 ± 5.27
AST (IU/L)	50.5 ± 30.0	59.9 ± 31.2	62.7 ± 48.1
ALT (IU/L)	56.0 ± 40.0	65.4 ± 42.7	77.7 ± 64.1
Total bilirubin (mg/dl)	0.66 ± 0.26	0.66 ± 0.19	0.55 ± 0.24
Albumin (g/dl)	4.08 ± 0.41	3.99 ± 0.43	4.07 ± 0.45
PT (%)	91.4 ± 15.0	90.2 ± 15.1	91.5 ± 15.1
Hyaluronic acid (ng/ml)	149.8 ± 218.0	155.3 ± 188.9	100.1 ± 99.9
Type 4 collagen 7S (ng/ml)	5.11 ± 2.01	5.28 ± 1.96	4.54 ± 0.84
AFP (ng/ml)	9.8 ± 20.4	14.2 ± 29.4	5.6 ± 4.2
APRI	0.90 ± 0.76	1.11 ± 0.94	1.04 ± 0.79
FIB4	2.80 ± 2.00	3.12 ± 2.25	2.93 ± 2.66
Vs value (m/sec)	1.39 ± 0.52	1.49 ± 0.56	1.35 ± 0.56

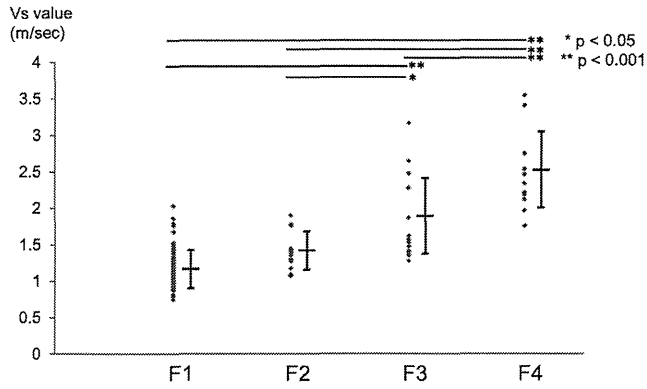

Fig. 1. Mean Vs values of each METAVIR fibrosis score *P*-value between F1 and F2 was 0.084.

Diagnostic Accuracy of ARFI for Liver Fibrosis

To assess the diagnostic accuracy of ARFI, the correlation between liver fibrosis and the Vs value by ARFI was evaluated for all 124 patients. The Vs value increased with the progression of the histological fibrosis stage, as assessed using the METAVIR scoring system, and a significant correlation was found between the two variables (Pearson product–moment correlation coefficient = 0.764, $P < 0.001$) (Fig. 1). There was a significant correlation between the Vs value and the following variables; platelet counts (Pearson product–moment correlation coefficient = −0.554, $P < 0.001$), alanine aminotransferase (ALT) (0.295, $P = 0.001$), total bilirubin (0.214, $P = 0.019$), albumin (−0.538, $P < 0.001$), hyaluronic acid (0.526, $P < 0.001$), type 4 collagen 7S (0.719, $P < 0.001$), and alpha-fetoprotein (0.556, $P < 0.001$). There was no significant correlation with the histological activity grade (0.171, $P = 0.058$) and HCV RNA (−0.039, $P = 0.672$). Next, the diagnostic ability of the Vs value for liver fibrosis was compared with the liver fibrosis formulae, such as APRI and FIB4, using the ROC values. The AUROCs of the Vs value, APRI and FIB4 for the diagnoses of moderate fibrosis (METAVIR fibrosis score ≥ F2) were 0.890, 0.779, and 0.737, respectively (Fig. 2A). There was a statistically significant difference between the Vs value and APRI ($P = 0.011$) and the Vs value and FIB4 ($P = 0.002$), according to the evaluation using the DeLong method. The cut-off value of the Vs value for moderate fibrosis was 1.26 m/sec (the sensitivity was 92.5%, the specificity was 76.2%, the PPV was 64.9%, and NPV was 95.5%, respectively). The diagnoses of severe fibrosis (METAVIR fibrosis score ≥ F3) were 0.943, 0.867, and 0.856 for Vs, APRI, and FIB4, respectively (Fig. 2B), and there were statistically significant differences between the Vs value and APRI ($P = 0.029$) and the Vs value and FIB4 ($P = 0.047$). Thus, ARFI showed a significantly higher diagnostic accuracy for liver fibrosis than that of the existing liver fibrosis formulae APRI and FIB4. The cut off value of the Vs value for severe fibrosis was 1.46 m/sec (the sensitivity was 84.6%, the specificity was 87.8%, the PPV was 64.7%, and NPV was 95.6%, respectively).

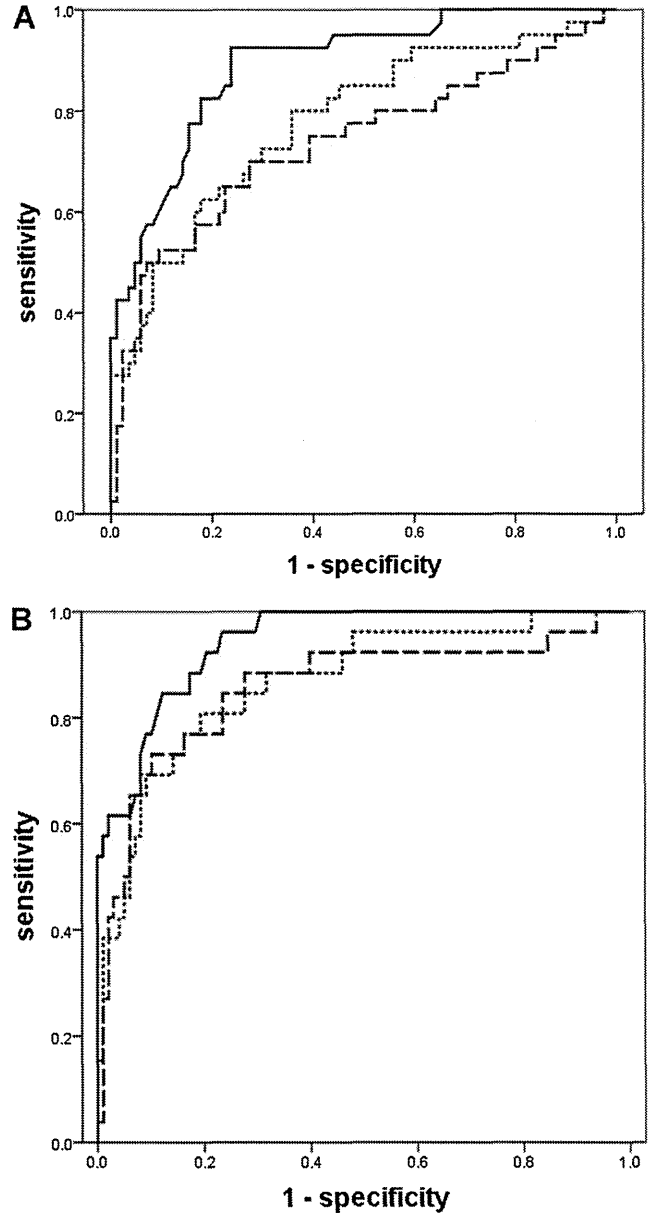

Fig. 2. Prognostic values of ARFI, APRI, and FIB4 for liver fibrosis. **A**: Discrimination ability for values higher than F2. AUC was 0.890 (95% CI: 0.830–0.949), 0.779 (0.688–0.870), and 0.737 (0.634–0.841), respectively. There was a significant difference between the Vs value and APRI ($P = 0.011$), and the Vs value and FIB4 ($P = 0.002$). **B**: Discrimination ability for values higher than F3. AUC was 0.943 (0.903–0.983), 0.867 (0.786–0.948), and 0.856 (0.759–0.953), respectively. There was a significant difference between the Vs value and APRI ($P = 0.029$), and the Vs value and FIB4 ($P = 0.047$). —, Vs value; --- APRI; ——— FIB4.

Association Between Vs Values and Treatment Response to Peg-IFN Plus Ribavirin Combination Therapy for Patients With Chronic Hepatitis C

Treatment response was assessed according to the HCV genotype among the patients who completed treatment. The baseline characteristics of these patients are shown in Table I. In all patients with HCV genotype 1, a complete early virologic response was obtained in 33% of the patients (15/46), a late virologic response in 28% (13/46), a non-virologic response in 39% (18/46), and a sustained virologic response in 54% (25/46). Table II shows the predictive factors affecting a sustained virologic response and a non-virologic response among genotype 1 patients elicited by the univariate analysis. In both analyses for predicting the treatment response, the IL28B genotype and Vs value showed a very strong impact on the treatment response (P values = 0.014 and 0.005, respectively, in the analysis of a sustained virologic response and 0.003 and 0.002, respectively, in the analysis of a non-virologic response). To evaluate the correlation between the Vs value and the treatment response, HCV genotype 1 patients were divided into two groups according to the baseline Vs value, with a mean value of 1.40 m/sec (Fig. 3A), and according to the IL28B genotype (Fig. 3B). A rapid virologic response was achieved in 15% (4/27) of patients with lower Vs values, but not in any patients with higher Vs values (0/19). The virologic response rates at week 12, end of treatment and at week 24 after the treatment were significantly higher in patients with relatively low Vs values compared with those of patients with higher Vs values ($P = 0.041$, $P = 0.001$, $P = 0.009$). The sustained virologic response rates were approximately twice as high in patients with low Vs values compared to patients with higher Vs values (70% (19/27) vs. 32% (6/19)). In a stratified analysis of the IL28B genotype,

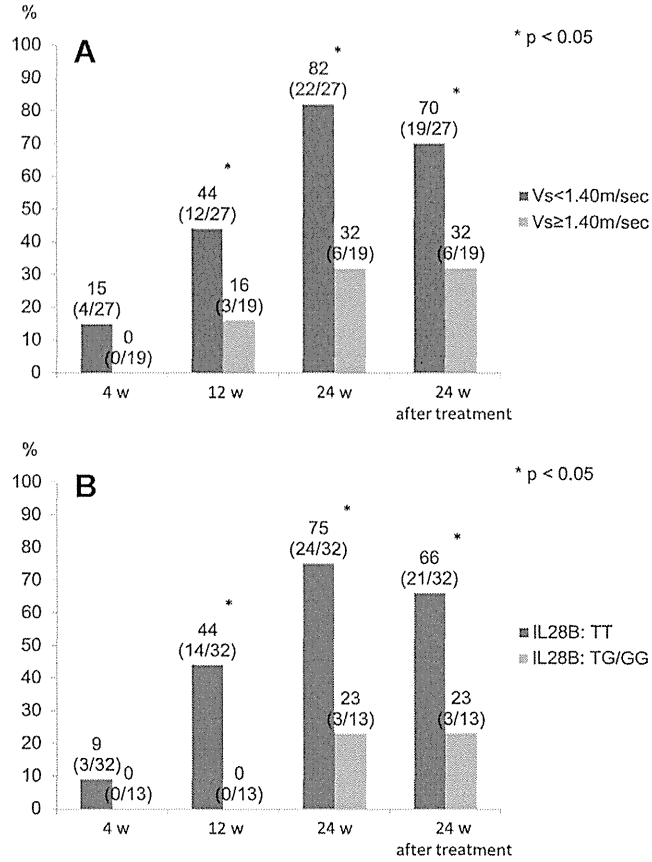

Fig. 3. HCV RNA-negative rates of all genotype 1 patients at week 4, week 12, week 24 and week 24 after the treatment (**A**) according to Vs value (Vs <1.40 m/sec vs. Vs ≥1.40 m/sec), (**B**) according to IL28B genotype (TT allele vs. TG/GG allele), *$P < 0.05$.

patients with the TT allele of IL28B had a significantly better treatment response than those with the TG/GG allele of IL28B (Fig. 3B). Concerning the IL28B genotype and Vs value, among patients with

TABLE II. Univariate Analysis for Predictive Factors Contributing to a Sustained Virologic Response and a Non-Virologic Response in Genotype 1

		Sustained virologic response			Non-virologic response		
Factor	Category	Odds ratio	95% CI	P-value	Odds ratio	95% CI	P-value
Gender	Male/female	0.509	0.148–1.747	0.283	1.294	0.375–4.468	0.683
Age (year)		0.869	0.788–0.959	0.005	1.060	0.992–1.133	0.084
BMI (kg/m^2)		1.009	0.855–1.190	0.920	1.044	0.882–1.236	0.617
IL28B SNP (rs8099917)	TT/TG/GG	0.157	0.036–0.692	0.014	10.000	2.191–45.639	0.003
Liver histology: fibrosis	F0/F1/F2/F3/F4	0.333	0.152–0.732	0.006	2.912	1.397–6.068	0.004
HCV-RNA (log IU/ml)		0.642	0.296–1.393	0.262	1.310	0.609–2.821	0.489
Platelet ($\times 10^4/\mu$l)		1.254	1.057–1.489	0.010	0.681	0.536–0.865	0.002
AST (IU/L)		0.985	0.966–1.005	0.149	1.023	1.001–1.045	0.038
ALT (IU/L)		0.996	0.982–1.010	0.542	1.009	0.994–1.024	0.222
Total bilirubin (mg/dl)		0.529	0.025–10.985	0.680	3.858	0.171–87.195	0.445
Albumin (g/dl)		1.609	0.402–6.451	0.502	0.248	0.054–1.149	0.075
PT (%)		1.050	1.002–1.101	0.042	0.929	0.877–0.984	0.012
AFP (ng/ml)		0.887	0.769–1.024	0.101	1.210	1.006–1.454	0.043
Baseline Vs value (m/sec)	By 0.1	0.778	0.654–0.926	0.005	1.336	1.112–1.604	0.002
Baseline Vs value (m/sec)	<1.40/≥1.40	0.194	0.054–0.693	0.012	9.533	2.421–37.541	0.001

the TT allele of IL28B, the rapid virologic response rate of patients with low Vs values was 16% (3/19), while that of patients with high Vs values was 0% (0/13). Furthermore, 54% (7/13) of patients with high Vs values showed no virologic response. Among patients with the TG/GG allele of IL28B, all patients with high Vs values experienced a non-virologic response during the 24 weeks of the treatment. Figure 4 shows the assessment of the predictive value of several metrics for the treatment response to peg-IFN plus ribavirin combination therapy. Among patients with the TT allele of IL28B, those with lower Vs values showed a high sustained virologic response rate (79%) (Fig. 4A) and had a significantly lower possibility of a non-virologic response than those with higher Vs values (5% vs. 54%, $P=0.003$) (Fig. 4B). Among patients with the TG/GG allele of IL28B, 43% (3/7) of the patients with low Vs values achieved a sustained virologic response (Fig. 4A), whereas all patients (6/6) with high Vs values showed a non-virologic response (Fig. 4B).

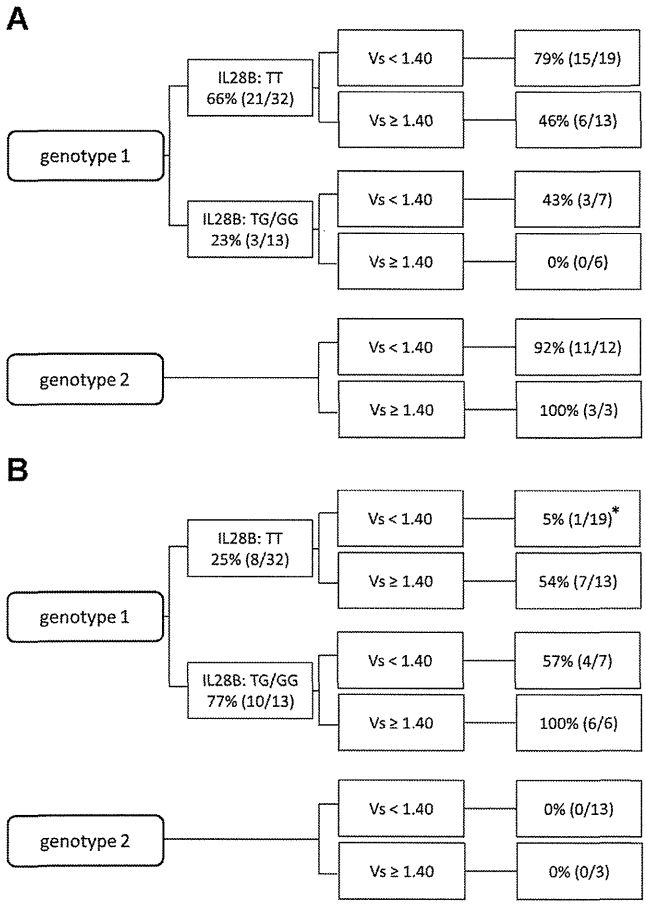

Fig. 4. Flowchart showing the possibility of treatment responses according to HCV genotype, IL28B genotype and Vs value. **A**: A sustained virologic response. **B**: A non-virologic response. Among genotype 1 patients with the TT allele of IL28B, those with higher Vs values showed a significantly higher non-virologic response rate than those with lower Vs values ($P=0.003$). Among genotype 2 patients, there were no significant differences between those with lower and higher Vs values in both the sustained virologic response rates and the non-virologic response rates.

In HCV genotype 2 patients, a sustained virologic response occurred in 93% (14/15) and there was no significant difference in the sustained virologic response rates between patients with low and high Vs values (92% vs. 100%, $P=0.800$) (Fig. 4A). Additionally, no patients showed a non-virologic response, irrespective of the degree of Vs values (Fig. 4B).

DISCUSSION

In the present study, the usefulness of ARFI, which is a non-invasive method, in the assessment of liver fibrosis was examined. The Vs value measured using ARFI had a significant correlation with the histological fibrosis stage estimated by the METAVIR fibrosis score. These values also showed higher diagnostic accuracy for liver fibrosis compared to the existing liver fibrosis formulae, such as APRI and FIB4. In addition to ARFI, Fibroscan® also provides quantitative measurements of tissue stiffness using ultrasound, and the AUC of Fibroscan® has been reported to be 0.76 for the diagnosis of moderate fibrosis (METAVIR fibrosis score $\geq$ F2). In this study, the AUC of ARFI was 0.89 for the diagnosis of moderate fibrosis. Thus, ARFI offers equivalent or higher diagnostic accuracy for liver fibrosis compared to Fibroscan®.

Next, the association between ARFI and treatment response in patients with chronic hepatitis C who received peg-IFN plus ribavirin combination therapy was investigated. For HCV genotype 1, patients with higher Vs values had low rates of a virologic response at week 24. This result was consistent with the prevailing notion that patients with advanced liver fibrosis are refractory to peg-IFN plus ribavirin combination therapy. On the other hand, the IL28B genotype is known to be a strong predictive factor contributing to the treatment response to peg-IFN plus ribavirin combination therapy, and the present study indicated that the treatment response could be predicted by determining both the IL28B genotype and the Vs value more precisely. Among patients with the TT allele of IL28B, which is the genotype that is generally recognized as favorable, those with lower Vs values showed a significantly higher treatment response than those with higher Vs values. Among patients with the TG/GG allele of IL28B, all patients (6/6) with higher Vs values exhibited a non-virologic response. Accordingly, it is important to consider the background of the patients with the TG/GG allele of IL28B and higher Vs values, including the probability of antiviral response, adverse effects and the risk of carcinogenesis, to judge the implementation of the present treatment. As new treatments using direct-acting antiviral agents (DAAs) are developed, it is essential to be able to predict a non-virologic response of existing antiviral therapies for patients with chronic hepatitis C.

In the present study, the Vs value was shown to be the most significant predictive factor for the antiviral response of peg-IFN plus ribavirin combination therapy. Indeed, although the METAVIR score is widely accepted as the gold standard to assess liver fibrosis, ARFI may be more generally applicable than liver histology because of its safe and uncomplicated method. In addition, ARFI presents the Vs value as a continuous variable and is a procedure with favorable reproducibility. Thus, objective and universal evaluations can be made.

The non-invasive method for assessing liver fibrosis by Fibroscan® is another option. However, a measurement obtained using Fibroscan® cannot indicate the exact area of the liver because this measurement is performed under M mode imaging. In contrast, the ARFI procedure can select the area of the liver using the ROI under B mode imaging and is rarely affected by obesity [Ebinuma et al., 2011]. Thus, the ARFI procedure may offer a higher advantage for diagnosing liver fibrosis than Fibroscan®.

In the present study, the diagnosis obtained using a combination of ARFI and IL28B data, both of which are obtained using non-invasive methods, was shown to be efficacious in the prediction of the antiviral response of peg-IFN plus ribavirin combination therapy for chronic hepatitis C patients with genotype 1. Patients with the TG/GG allele of IL28B and high Vs values were considered refractory to standard therapy.

ACKNOWLEDGMENT

We are grateful to all study participants, especially for Shinichi Kiso and Akinori Kasahara.

REFERENCES

Bedossa P, Poynard T. 1996. An algorithm for the grading of activity in chronic hepatitis C. The METAVIR Cooperative Study Group. Hepatology 24:289–293.

Degos F, Perez P, Roche B, Mahmoudi A, Asselineau J, Voitot H, Bedossa P. 2010. Diagnostic accuracy of FibroScan and comparison to liver fibrosis biomarkers in chronic viral hepatitis: A multicenter prospective study (the FIBROSTIC study). J Hepatol 53:1013–1021.

Ebinuma H, Saito H, Komuta M, Ojiro K, Wakabayashi K, Usui S, Chu PS, Umeda R, Ishibashi Y, Takayama T, Kikuchi M, Nakamoto N, Yamagishi Y, Kanai T, Ohkuma K, Sakamoto M, Hibi T. 2011. Evaluation of liver fibrosis by transient elastography using acoustic radiation force impulse: Comparison with Fibroscan((R)). J Gastroenterol 46:1238–1248.

Everson GT, Hoefs JC, Seeff LB, Bonkovsky HL, Naishadham D, Shiffman ML, Kahn JA, Lok AS, Di Bisceglie AM, Lee WM, Dienstag JL, Ghany MG, Morishima C. 2006. Impact of disease severity on outcome of antiviral therapy for chronic hepatitis C: Lessons from the HALT-C trial. Hepatology 44:1675–1684.

Fried MW, Shiffman ML, Reddy KR, Smith C, Marinos G, Goncales FL, Jr., Haussinger D, Diago M, Carosi G, Dhumeaux D, Craxi A, Lin A, Hoffman J, Yu J. 2002. Peginterferon alfa-2a plus ribavirin for chronic hepatitis C virus infection. N Engl J Med 347:975–982.

Friedrich-Rust M, Wunder K, Kriener S, Sotoudeh F, Richter S, Bojunga J, Herrmann E, Poynard T, Dietrich CF, Vermehren J, Zeuzem S, Sarrazin C. 2009. Liver fibrosis in viral hepatitis: Noninvasive assessment with acoustic radiation force impulse imaging versus transient elastography. Radiology 252:595–604.

Hadziyannis SJ, Sette H, Jr., Morgan TR, Balan V, Diago M, Marcellin P, Ramadori G, Bodenheimer H, Jr., Bernstein D, Rizzetto M, Zeuzem S, Pockros PJ, Lin A, Ackrill AM. 2004. Peginterferon-alpha2a and ribavirin combination therapy in chronic hepatitis C: A randomized study of treatment duration and ribavirin dose. Ann Intern Med 140:346–355.

Hiramatsu N, Hayashi N, Kasahara A, Hagiwara H, Takehara T, Haruna Y, Naito M, Fusamoto H, Kamada T. 1995. Improvement of liver fibrosis in chronic hepatitis C patients treated with natural interferon alpha. J Hepatol 22:135–142.

Ishak K, Baptista A, Bianchi L, Callea F, De Groote J, Gudat F, Denk H, Desmet V, Korb G, MacSween RN, Phillips J, Portmannl BG, Paulsen H, Scheuer PJ, Schmid M, Thaler S. 1995. Histological grading and staging of chronic hepatitis. J Hepatol 22:696–699.

Kasahara A, Hayashi N, Mochizuki K, Takayanagi M, Yoshioka K, Kakumu S, Iijima A, Urushihara A, Kiyosawa K, Okuda M, Hino K, Okita K. 1998. Risk factors for hepatocellular carcinoma and its incidence after interferon treatment in patients with chronic hepatitis C. Osaka Liver Disease Study Group. Hepatology 27:1394–1402.

Kasahara A, Tanaka H, Okanoue T, Imai Y, Tsubouchi H, Yoshioka K, Kawata S, Tanaka E, Hino K, Hayashi K, Tamura S, Itoh Y, Kiyosawa K, Kakumu S, Okita K, Hayashi N. 2004. Interferon treatment improves survival in chronic hepatitis C patients showing biochemical as well as virological responses by preventing liver-related death. J Viral Hepat 11:148–156.

Kurokawa M, Hiramatsu N, Oze T, Mochizuki K, Yakushijin T, Kurashige N, Inoue Y, Igura T, Imanaka K, Yamada A, Oshita M, Hagiwara H, Mita E, Ito T, Inui Y, Hijioka T, Yoshihara H, Inoue A, Imai Y, Kato M, Kiso S, Kanto T, Takehara T, Kasahara A, Hayashi N. 2009. Effect of interferon alpha-2b plus ribavirin therapy on incidence of hepatocellular carcinoma in patients with chronic hepatitis. Hepatol Res 39:432–438.

Manns MP, McHutchison JG, Gordon SC, Rustgi VK, Shiffman M, Reindollar R, Goodman ZD, Koury K, Ling M, Albrecht JK. 2001. Peginterferon alfa-2b plus ribavirin compared with interferon alfa-2b plus ribavirin for initial treatment of chronic hepatitis C: A randomised trial. Lancet 358:958–965.

Oze T, Hiramatsu N, Yakushijin T, Mochizuki K, Imanaka K, Yamada A, Oshita M, Kaneko A, Hagiwara H, Mita E, Ito T, Nagase T, Inui Y, Hijioka T, Tamura S, Yoshihara H, Hayashi E, Imai Y, Kato M, Hosui A, Miyagi T, Yoshida Y, Ishida H, Tatsumi T, Kiso S, Kanto T, Kasahara A, Takehara T, Hayashi N. 2011. The efficacy of extended treatment with pegylated interferon plus ribavirin in patients with HCV genotype 1 and slow virologic response in Japan. J Gastroenterol 46:944–952.

Sterling RK, Lissen E, Clumeck N, Sola R, Correa MC, Montaner J, SS M, Torriani FJ, Dieterich DT, Thomas DL, Messinger D, Nelson M. 2006. Development of a simple noninvasive index to predict significant fibrosis in patients with HIV/HCV coinfection. Hepatology 43:1317–1325.

Tanaka Y, Nishida N, Sugiyama M, Kurosaki M, Matsuura K, Sakamoto N, Nakagawa M, Korenaga M, Hino K, Hige S, Ito Y, Mita E, Tanaka E, Mochida S, Murawaki Y, Honda M, Sakai A, Hiasa Y, Nishiguchi S, Koike A, Sakaida I, Imamura M, Ito K, Yano K, Masaki N, Sugauchi F, Izumi N, Tokunaga K, Mizokami M. 2009. Genome-wide association of IL28B with response to pegylated interferon-alpha and ribavirin therapy for chronic hepatitis C. Nat Genet 41:1105–1109.

Toshima T, Shirabe K, Takeishi K, Motomura T, Mano Y, Uchiyama H, Yoshizumi T, Soejima Y, Taketomi A, Maehara Y. 2011. New method for assessing liver fibrosis based on acoustic radiation force impulse: A special reference to the difference between right and left liver. J Gastroenterol 46:705–711.

Wai CT, Greenson JK, Fontana RJ, Kalbfleisch JD, Marrero JA, Conjeevaram HS, Lok AS. 2003. A simple noninvasive index can predict both significant fibrosis and cirrhosis in patients with chronic hepatitis C. Hepatology 38:518–526.

Pathogens **2014**, *3*, 377-389; doi:10.3390/pathogens3020377

OPEN ACCESS

pathogens

ISSN 2076-0817

www.mdpi.com/journal/pathogens

Review

Mouse Models of Hepatitis B Virus Infection Comprising Host-Virus Immunologic Interactions

Tadashi Inuzuka, Ken Takahashi, Tsutomu Chiba and Hiroyuki Marusawa *

Department of Gastroenterology and Hepatology, Graduate School of Medicine, Kyoto University, 54 Shogoin-Kawahara-cho, Sakyo-ku, Kyoto 606-8103, Japan; E-Mails: tinuzuka@kuhp.kyoto-u.ac.jp (T.I.); takaken@kuhp.kyoto-u.ac.jp (K.T.); chiba@kuhp.kyoto-u.ac.jp (T.C.)

* Author to whom correspondence should be addressed; E-Mail: maru@kuhp.kyoto-u.ac.jp; Tel.: +81-75-751-4319; Fax: +81-75-751-4303.

Received: 6 March 2014; in revised form: 9 April 2014 / Accepted: 11 April 2014 / Published: 23 April 2014

Abstract: Hepatitis B virus (HBV) infection is one of the most prevalent infectious diseases associated with various human liver diseases, including acute, fulminant and chronic hepatitis; liver cirrhosis; and hepatocellular carcinoma. Despite the availability of an HBV vaccine and the development of antiviral therapies, there are still more than 350 million chronically infected people worldwide, approximately 5% of the world population. To understand the virus biology and pathogenesis in HBV-infected patients, several animal models have been developed to mimic hepatic HBV infection and the immune response against HBV, but the narrow host range of HBV infection and lack of a full immune response spectrum in animal models remain significant limitations. Accumulating evidence obtained from studies using a variety of mouse models that recapitulate hepatic HBV infection provides several clues for understanding host-virus immunologic interactions during HBV infection, whereas the determinants of the immune response required for HBV clearance are poorly defined. Therefore, adequate mouse models are urgently needed to elucidate the mechanism of HBV elimination and identify novel targets for antiviral therapies.

Keywords: animal model; transgenic mouse; humanized mouse; immune response

1. Introduction

Hepatitis B virus (HBV), a member of the Hepadnaviridae family, is an enveloped, circular, single-stranded, and partially double-stranded DNA virus that causes acute and chronic liver disease and hepatocellular carcinoma [1,2]. More than 350 million people worldwide, approximately 5% of the world population, are chronically infected with HBV [3]. Despite our deepening understanding of the pathophysiology of HBV infection, the precise molecular mechanisms of the viral life cycle, persistence of infection, and associated carcinogenesis remain unclear. To understand the pathogenesis caused by HBV infection, adequate animal models that recapitulate HBV-associated liver disease are required. Establishing animal models of HBV infection is difficult as HBV has a narrow host range and exclusively infects humans. Chimpanzees and, to a certain extent, tupaia, the Asian tree shrew, have been used for experimental infection [4,5]. The chimpanzee is the only immunocompetent host fully susceptible to HBV infection, as demonstrated by the induction of acute hepatitis after injection of serum from human HBV carriers [6]. Their large size, associated strong ethical constraints, and the high cost of chimpanzees are increasingly restricting their use for research of human hepatotropic viruses. Although HBV infects tupaias, it causes only mild and transient infection with low viral titers, despite viral DNA replication in the liver, HBsAg secretion into the serum, and the production of antibodies to HBsAg and HBeAg [5]. In addition, tupaias are relatively large animals, difficult to handle in captivity, and not easily available. They are all of outbred origin and their immune systems have not been characterized. Thus, due to the various restrictions for using the currently available models of hepadnavirus infection, and the necessity to work in a well-defined, inbred, and small animal system, most recent developments have focused on mice. Many researchers have attempted to develop mouse models of HBV infection of human livers (Table 1). This review focuses on the history of the currently available mouse models for HBV research to clarify the current status and future directions.

Table 1. Comparison of the currently available animal model systems for HBV infection.

Animal model	Advantages	Disadvantages
Human	Natural target of infection	
Chimpanzee	An immunocompetent host fully susceptible to HBV infection, similar to human infection (including cccDNA)	Ethical constraints, large size, high costs, transient infection
Tupaia	Susceptible to HBV infection, similar to human infection (including cccDNA)	Relatively large size, not easily available, outbred animals, transient infection
Mouse	Small, inbred animals, genetically and immunologically well-known	No-infection
Transgenic mouse	convenient, inbred animals, immunological experiment with adoptive transfer	No-infection, immune tolerance

Table 1. *Cont.*

Animal model	Advantages	Disadvantages
Transfected mouse by hydrodynamic injection	Analysis of mutant strains, immunocompetent	No-infection, transient gene expression,
Transfected mouse by adeno-associated virus	High replication levels, analysis of mutant strains, immunocompetent, relatively long-time gene-expression	No-infection, transient gene expression, possible vector-driven interferences
Human liver-chimeric mouse	Susceptible to HBV infection (including cccDNA), capable to use clinical specimen, assessment of efficacy of anti-HBV agents	high costs, immunocompromised, Transient infection (but relatively long infection)

2. Mouse Models

2.1. HBV-Transgenic Mouse Models

After extensive effort, Chisari *et al.* and other groups developed HBV transgenic mice that express the HBV envelope [7–9], core [10,11], precore [12], or X [13,14] gene products. These mice provide the opportunity to analyze heretofore undescribed aspects of HBV virology, such as assembly, transport, secretion, and host immune response to HBV. These models, however, are limited in that they express only a single viral-encoded protein and thus viral replication is not analyzable. To overcome this problem, transgenic mice in which HBV replicates in murine hepatocytes were developed. Araki *et al.* first developed transgenic mice using a construct capable of transcribing all viral genes and observed low levels of HBV replication in the liver as well as the production of HBsAg and HBeAg [15]. Thereafter, transgenic mice with terminally redundant over-length 1.3 HBV-DNA insertion, which produces viral particles at high levels comparable to those of chronic hepatitis patients, were developed [16]. The virions produced in these mice are morphologically indistinguishable from human-derived virions [16] and are infectious when inoculated into chimpanzees [17]. This model, with its advantage of very-high-level HBV replication, provides the opportunity to dissect mechanisms of the viral life cycle and HBV immunobiology, and assess the efficacy of anti-HBV agents (see Figure 1). Although a comprehensive review of the knowledge gained from research using this series of transgenic mice is not possible in this limited review, we present representative studies of these model mice.

First, studies using HBV transgenic mice have elucidated that HBV is not directly cytopathic for hepatocytes and that both disease pathogenesis and viral clearance are mediated by an antiviral adaptive immune response to HBV [16]. Pathogenic functions of adaptive immunity were demonstrated by the observation that adoptive transfer of HBV-antigen specific cytotoxic T cells (CTLs) to HBV transgenic mice causes acute necroinflammatory liver disease in these mice in which HBV replication itself shows no cytopathic effect [18]. The most important finding in this disease model was that antigen-specific CTLs not only cause hepatocellular injury but also noncytopathically inhibit HBV gene expression and viral replication [18]. Viral clearance is completely blocked by

antibodies to interferon (IFN)-γ, and tumor necrosis factor (TNF)-α, indicating that these cytokines are responsible for the noncytopathic antiviral effect of CTLs. The importance of CTLs in the disease pathogenesis and viral clearance was further confirmed by studies of HBV-infected chimpanzees [19]. Antibody-mediated depletion of CTLs delays the onset of viral clearance and liver disease until HBV-specific CTLs become detectable again with the decreasing antibody titer. Together, these findings led to the concept that viral clearance during HBV infection is essentially mediated by noncytolytic mechanisms of CTLs and that liver disease caused by cytolytic mechanisms is an unfavorable side effect of CTL activation. In addition, further studies on HBV transgenic mice revealed that the antigen-nonspecific inflammatory cells exacerbate CTL-induced liver immunopathology and that platelets contribute to both liver disease and viral clearance by facilitating the accumulation of CTLs in the inflamed liver, uncovering the highly complex but coordinated nature of host-viral interaction [20–25]. Second, HBV transgenic mice are a powerful tool for evaluating the impact of antiviral cytokines or anti-HBV drugs. Indeed, HBV replication is inhibited by IFN-α, IFN-β, or IFN-γ induced by innate or adaptive immune cells [26,27] and the efficacy of nucleoside analogs, lamivudine [28], adefovir dipivoxil [29] and entecavir [30], has been demonstrated in HBV-transgenic mice. Small interfering RNAs (siRNAs) specifically targeting HBV RNA transcripts suppress HBV replication in the HBV transgenic mice [31,32]. Furthermore, 5'-triphosphorylated HBV-specific siRNAs that are capable of activating the retinoid acid-inducible protein I-dependent pathway more efficiently control HBV by the dual mechanisms of direct suppression of the viral gene expression and induction of an intrahepatic type I IFN response [33].

Figure 1. Hepatitis B virus (HBV) transgenic mouse model.

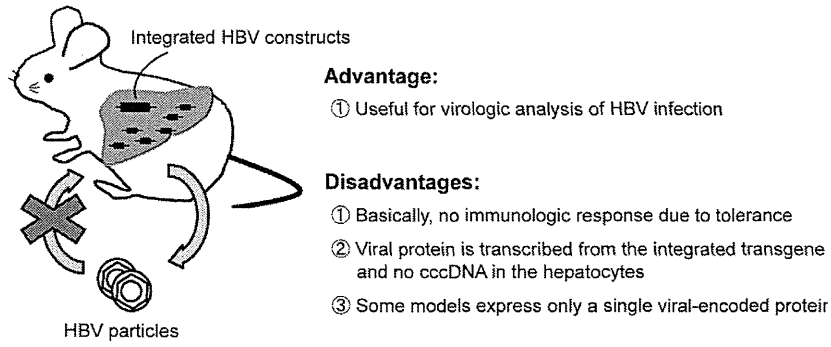

Although no one doubts that HBV transgenic mouse model has greatly expanded our knowledge of hepatitis B, several limitations of this model must be taken into account. First, HBV particles produced by the transgenic mice do not enter into murine hepatocytes, which lack HBV-specific receptors [34]. Researchers thus cannot study the infection step of the HBV life cycle. Second, covalently closed circular DNA (cccDNA) is not detected in the liver of HBV transgenic mice. This cannot be dismissed, because cccDNA, the template of viral transcription in natural infection, could be an important therapeutic target to achieve complete eradication of HBV [35,36]. Finally, due to the immunotolerant nature of HBV transgenic mice, the mice do not develop hepatitis per se and only downstream events after adoptive transfer of *in vitro*-stimulated HBV-antigen specific CTLs are analyzable, which prevents comprehensive understanding of the immune response to HBV. This limitation, however, was

partially overcome by the newly developed HBV transgenic mouse model, where T and B cell adaptive immune system was ablated by crossing HBV transgenic mice with *Rag1*-deficient mice [37,38]. In this model, adoptive transfer of HBV-naïve splenocytes to adult but not young transgenic mice resulted in the spontaneous development of effective immune response to HBV with concomitant liver disease. With the advantage that naïve immune system is primed to viral antigen originating in the liver, this model is suitable for the analysis of immune-priming event and has provided the opportunity to dissect the age-dependent immunological differences in HBV clearance and persistence [37,38].

2.2. HBV Transfection by Hydrodynamic Injection

Because transgenic mice are immunologically tolerant to the virus, it is difficult to study the host immune response and the resultant pathophysiology of HBV infection. To overcome this problem, several researchers applied the transient expression of HBV protein in the liver of adult mice using hydrodynamic injection techniques (see Figure 2) [39,40]. Hydrodynamic injection techniques involve rapid injection of a high volume of fluids containing naked DNA encoding partial or full-length HBV genome sequences into the tail vein of mice. Hydrodynamic injection of a naked plasmid DNA encoding a supergenomic HBV 1.3-length transgene into inbred mice could induce high levels of HBV replication in the liver, producing circulating HBV DNA at levels of 8×10^6 copies/mL blood. HBV replication in the liver, however, is rapidly terminated within 15 days after injection by specific antiviral antibodies and CTLs if the mice are immunocompetent. In contrast, the virus persists over 80 days after hydrodynamic injection in immunodeficient NOD/scid mice lacking functional B-, T-lymphocytes, and natural killer cells [39]. This experimental approach using a panel of immunodeficient mouse strains for the examination of anti-HBV immunologic responses clarified that hepatic clearance of the input HBV templates requires a variety of effectors, including CD4+ and CD8+ T cells, natural killer cells, Fas, IFN-gamma (IFN-γ), IFN-alpha/beta receptor (IFN-α/βR1), and TNF receptor 1 (TNFR1) [41]. On the other hand, B cells and perforin are not essential for clearance of the HBV transcriptional template from the liver in the hydrodynamically-transfected mouse model. Based on those findings, CTLs (CD8+ T cells) are thought to be the key cellular effectors mediating HBV clearance from the liver by a Fas-dependent, but perforin independent, process in which natural killer cells, IFN-γ, TNFR1, and IFN-α/βR play supporting roles, suggesting the existence of redundant pathways that inhibit HBV replication [41]. Thus, at present, in addition to the adaptive immune system like CD4+ and CD8+ T cells, it is thought that the innate immune system also plays an important role in HBV-induced liver inflammation and disease progression [42].

2.3. HBV Transfection by Adeno-Associated Virus

Recently, another mouse model of HBV replication was newly developed. Dion *et al.* described a mouse model that allows the HBV persistence based on the liver-targeted transduction of adeno-associated virus serotype 2/8 (AAV2/8), which delivered the HBV genome enabling the study of viral infection for up to one year [43]. In this model, hepatitis B core antigen (HBcAg) expression was detected in approximately 60% of hepatocytes, contrasting with the 5 to 10% of hepatocytes with HBcAg expression achieved by the hydrodynamic injection of conventional plasmids encoding HBV

genome. In addition, AAV allows homogeneous transduction of the liver, whereas not all parts of the liver are reached after hydrodynamic injection [39]. This mouse model recapitulates virological and immunological characteristics of chronic HBV infection, and could be useful for the development of new treatment and immune-based therapies or therapeutic vaccines for chronic HBV infections [43,44].

Figure 2. Hydrodynamic injection model.

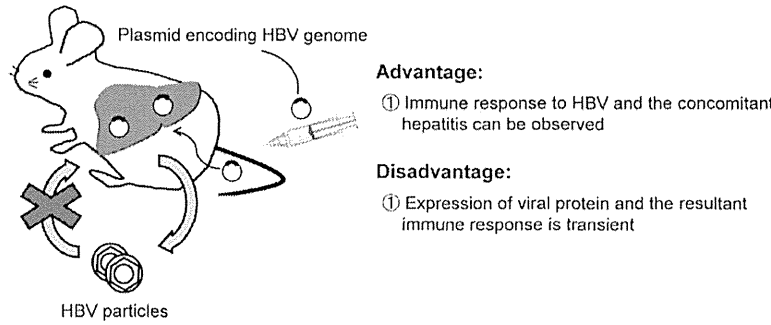

2.4. Chimeric Mouse Models of HBV Infection

As described above, HBV transgenic mouse models have had important roles for clarifying the pathophysiology of the host immune response to HBV. Because HBV does not infect the murine hepatocytes, these mice do not recapitulate natural HBV infection. To overcome these problems, researchers have attempted to transplant human hepatocytes into mice. The development of the trimera mouse was one result of such an attempt, in which human hepatocytes were transplanted under the kidney capsule of immunodeficient mice after lethal irradiation [45]. The number of hepatocytes that could survive on the kidney capsule was small, however, and the normal liver architecture was not observed. Although 85% of transplanted mice developed HBV viremia, the titer was less than 10^5 virus particles or IU/mL and lasted only ~20 days [45].

To establish HBV infection in mice, two human-liver chimeric mouse models were developed. The first was the urokinase-type plasminogen activator (uPA)/scid mouse, which remains the most widely model used for infection studies and preclinical drug evaluation. Transgenic mice in which the urokinase gene expression is driven by the human albumin promoter/enhancer (uPA mice) show accelerated hepatocyte death with consequent chronic hepatocyte growth stimulation [46]. Transplanted rat hepatocytes proliferate and repopulate in the injured livers of immunodeficient uPA mice, which are produced by mating uPA transgenic mice with scid mice (uPA/scid mice) [47]. Human hepatocytes transplanted into uPA/scid mice were demonstrated to successfully proliferate and replace apoptotic murine hepatocytes. [48–50]. The disadvantages of uPA/scid mice are infertility and susceptibility to fatal hemorrhaging [46,51]. The second model was a $Fah^{-/-}Rag2^{-/-}Il2rg^{-/-}$ mouse, deficient in fumarylacetoacetate hydrolase (Fah), recombination activating gene 2 (Rag2), and gamma-chain of the receptor for IL-2 (Il2rg). Fah is the last enzyme in the tyrosine breakdown pathway, and its deficiency leads to liver failure in mice. Treatment with 2-(2-nitro-4-trifluoromethylbenzyol)-cyclohexane-1, 3-dione (NTBC) prevents the accumulation of toxic metabolites and the resultant hepatotoxicity. Induction of liver injury by the withdrawal of NTBC allows for successful transplantation of human hepatocytes with high rates of chimerism [52,53].